JARO 14: 843–862 (2013)
DOI: 10.1007/s10162-013-0412-1

JARO
Journal of the Association for Research in Otolaryngology

Research Article

Stimulus-Frequency Otoacoustic Emission Suppression Tuning in Humans: Comparison to Behavioral Tuning

Karolina K. Charaziak,[1] Pamela Souza,[1] and Jonathan H. Siegel[1]

[1]*Department of Communication Sciences and Disorders, Northwestern University, School of Communication, 2240 Campus Drive, Evanston, IL 602080-2952, USA*

Received: 18 June 2012; Accepted: 11 August 2013; Online publication: 7 September 2013

ABSTRACT

As shown by the work of Kemp and Chum in 1980, stimulus-frequency otoacoustic emission suppression tuning curves (SFOAE STCs) have potential to objectively estimate behaviorally measured tuning curves. To date, this potential has not been tested. This study aims to do so by comparing SFOAE STCs and behavioral measures of tuning (simultaneous masking psychophysical tuning curves, PTCs) in 10 normal-hearing listeners for frequency ranges centered around 1,000 and 4,000 Hz at low probe levels. Additionally, SFOAE STCs were collected for varying conditions (probe level and suppression criterion) to identify the optimal parameters for comparison with behavioral data and to evaluate how these conditions affect the features of SFOAE STCs. SFOAE STCs qualitatively resembled PTCs: they demonstrated band-pass characteristics and asymmetric shapes with steeper high-frequency sides than low, but unlike PTCs they were consistently tuned to frequencies just above the probe frequency. When averaged across subjects the shapes of SFOAE STCs and PTCs showed agreement for most recording conditions, suggesting that PTCs are predominantly shaped by the frequency-selective filtering and suppressive effects of the cochlea. Individual SFOAE STCs often demonstrated irregular shapes (e.g., "double-tips"), particularly for the 1,000-Hz probe, which were not observed for the same subject's PTC. These results show the limited utility of SFOAE STCs to assess tuning in an individual. The irregularly shaped SFOAE STCs may be attributed to contributions from SFOAE sources distributed over a region of the basilar membrane extending beyond the probe characteristic place, as suggested by a repeatable pattern of SFOAE residual phase shifts observed in individual data.

Keywords: frequency selectivity, normal hearing, psychophysical tuning curve

Correspondence to: Karolina K. Charaziak • Department of Communication Sciences and Disorders • Northwestern University, School of Communication • 2240 Campus Drive, Evanston, IL 602080-2952, USA. Telephone: +1-847-4912463; fax: +1-708-4912523; email: KarolinaCharaziak2013@u.northwestern.edu

INTRODUCTION

Otoacoustic emissions (OAEs), sounds generated by healthy ears, have been used as noninvasive probes of cochlear function (for review see Robinette and Glattke 2007). However, their clinical applications remain limited due to uncertainty about mechanisms of OAE generation (e.g., Shera 2004; Siegel et al. 2005; Johnson 2010) and difficulties relating OAEs to behavioral tests of hearing (for review see Johnson et al. 2007). Here, we address the latter issue by comparing behavioral and single-tone OAEs (stimulus-frequency otoacoustic emissions, SFOAEs) tuning measured with analogous paradigms in the same ear. We aim to determine whether SFOAE can provide information about tuning (related to auditory frequency selectivity) equivalent to that obtained with psychophysical tuning curves (PTCs) in adults with normal hearing.

Frequency selectivity refers to the ability of the auditory system to separate one stimulus out from others on the basis of frequency (Moore 2004) which is important for perception of complex sounds, such as music and speech, as well as hearing in noise

(reviewed in Moore 2007). Frequency selectivity is largely determined at the level of the cochlea (e.g., Evans 2001) where outer hair cells provide sharp mechanical tuning at low signal levels (e.g., Rhode 1971; for review see Ruggero and Rich 1991). In humans, frequency selectivity is most often measured using auditory masking (e.g., Fletcher 1940; Vogten 1974; Patterson 1976; Oxenham and Shera 2003). One method is to measure a PTC, where the threshold of audibility of a fixed low level (i.e., 10 dB SL) probe tone is measured as a function of the frequency of a masker (tone or band of noise), forming a characteristic "V" shaped curve (Zwicker 1974). The masker and the probe can be presented simultaneously or separated in time (e.g., forward masking paradigm). It is a matter of debate which behavioral paradigm is the best approach for assessing *cochlear* frequency selectivity (e.g., Houtgast 1972; Pickles 1979; Evans 2001; Oxenham and Shera 2003; Ruggero and Temchin 2005). In the simultaneous masking paradigm, both spread of excitation and suppression effects are believed to contribute to the observed masking (Pickles 1984; Delgutte 1990b; Gifford and Bacon 2000; Rodriguez et al. 2010). The contribution of suppression may result in underestimation of cochlear frequency selectivity measured directly with neural or basilar membrane single-tone tuning curves (Sachs and Kiang 1968; Sellick and Russell 1979; Rhode 2007). Nevertheless, it is generally agreed that this type of masking paradigm provides useful information about frequency selective sound processing in the auditory system (Oxenham and Shera 2003).

The simultaneous masking PTC paradigm closely mimics the OAE suppression tuning curve (STC) measure, where a fixed change in the OAE amplitude is tracked across suppressor frequencies. If OAE STCs provide a measure of auditory tuning equivalent to PTCs, then the advantage of this objective and fast procedure would be attractive. Multiple studies indicate that OAE STCs qualitatively resemble behavioral tuning curves in humans for all types of emissions (e.g., Kemp and Chum 1980; Zurek 1981; Zwicker and Wesel 1990; Harris et al. 1992). However, the commonly studied distortion-product (DP) OAE STCs seem to underestimate frequency selectivity (Koppl and Manley 1993; Taschenberger and Manley 1998; Gorga et al. 2002; Johnson et al. 2007; Liu and Neely 2013), possibly due to the proposed two-source generation mechanism of DPOAEs (Shera and Guinan 1999; Knight and Kemp 2001) and/or a broad region of generation (Martin et al. 2010). On the other hand, OAEs that are believed to arise *via* a single mechanism, i.e., SFOAEs, transient-evoked (TE) OAEs and spontaneous (S) OAEs, appear to be a better alternative for assessing frequency selectivity because they may provide a more localized picture of cochlear processes than DPOAEs (Zweig and Shera 1995; Shera and Guinan 1999; Talmadge et al. 2000). Although tuning data are sparse for these types of emissions, a few reports indicate a good match between either SOAE, TEOAE or SFOAE STCs and behavioral estimates of frequency selectivity for humans (e.g., Kemp and Chum 1980; Zurek 1981; Schloth and Zwicker 1983; Long 1984; Rabinowitz and Widin 1984; Bargones and Burns 1988; Zizz and Glattke 1988; Zwicker and Wesel 1990; Long et al. 1991; Zettner and Folsom 2003; Keefe et al. 2008). Further support for use of single-source OAE STCs to estimate tuning comes from animal studies. It has been shown that SFOAE STCs can be as sharply tuned as auditory nerve tuning curves in mice (Cheatham et al. 2011) and SOAE STCs have tuning characteristics similar to auditory-nerve fiber tuning curves in reptiles and birds (Koppl and Manley 1994; Taschenberger and Manley 1997). However, whether SFOAE STCs may quantitatively predict behavioral tuning in humans remains an open question.

In summary, single-source OAE STCs may provide an accurate measure of behavioral tuning in humans. To test this hypothesis, we measured SFOAE STCs together with PTCs in normal hearing subjects. We decided to focus on SFOAEs because they are evoked by the same stimulus (single tone) as used in the behavioral PTC measurements. The tuning curves were collected at low probe levels (10 dB SL) to ensure that active cochlear processes would contribute fully to sharp tuning. SFOAE STCs were collected with varying suppression criteria as well as for slightly higher probe levels (20 and 30 dB SL) to form a basis to optimize estimates of tuning in a broader population (i.e., hearing-impaired subjects or subjects with inadequate SFOAE levels for low-level stimuli). Before we compared SFOAE STCs to PTCs, we also evaluated the effects and interactions of changing the probe level and suppression criteria on the features of SFOAE STCs to better understand how these curves were shaped by the cochlear processes.

MATERIALS AND METHODS

Subjects

Ten young, normal-hearing subjects (19–24 years old, 7 females) with no history of neural or otologic disorders participated in the study. No subjects reported a history of noise exposure or difficulty with hearing in noise. All subjects had hearing thresholds within 15 dB of mean thresholds for normal hearing young adults at octave frequencies between 250 and 8,000 Hz (Lee et al. 2012), normal middle ear status (assessed via 226-Hz tympanometry, Interacoustics, AA220; Margolis and

Heller 1987) and normal results of otoscopic examination. To be included in the study, a subject had to demonstrate an SFOAE residual level of −6 dB SPL or higher (with SNR>6 dB) at least at one frequency near 1,000 Hz and near 4,000 Hz when stimulated at low probe levels (see SFOAE "fine structure" recordings in Procedures). No detectable SOAE could be present within ±350 Hz around the probe frequency.

The study was approved by the Northwestern University Institutional Review Board and subjects were paid an hourly rate for their participation.

Instrumentation

All measurements were carried out in a sound-attenuating booth. The signals were generated and controlled with software (see the "Procedures" section) using a 24-bit audio interface (Echo Audio Gina3G). The sound source transducers were modified MB Quart 13.01 HX coupled to an Etymotic Research ER10-B+ otoacoustic emission probe via flexible 16 ga plastic tubing. The tonal stimuli and the suppressor or masker were presented monaurally through separate sound sources to minimize nonlinear stimulus interactions. The power amplifier used to drive the sound sources was custom-built, using a Texas Instruments TPA6120A2 headphone driver IC with a dynamic range of 120 dB. Tones were generated digitally by the audio interface with a sample rate of 44.1 kHz (buffer size 8,192 points, frequency resolution of 5.31 Hz) for data collected with Emav software (Neely and Liu 2011) and with a sample rate of 88.2 kHz (4,096 points, frequency resolution of 21.53 Hz) for the custom made software. The microphone transfer function was measured as described by Siegel (2007) and used to compensate the measured stimulus and emission signals. The stimulus level at the subject's eardrum was controlled using the depth-compensated ear simulator method (Lee et al. 2012). For PTC measurements, the masker level at the eardrum was calculated offline.

The biological origin of OAEs was confirmed by running the test protocols in an ear simulator (IEC 60318–4; Brüel & Kjær 4157).

Procedures

Data for each subject were usually collected within four 2-h sessions. Two subjects were tested twice to assess the test–retest repeatability of the acquired measures. Typically, an SFOAE STC was collected within 10–15 min, and a PTC within 4 min.

Behavioral Thresholds

Air-conduction hearing thresholds were obtained with a modified Békésy tracking procedure (as described by Lee et al. 2012). Briefly, stimuli were tones, 500 ms in duration with 25 ms rise/fall times, and interstimulus interval of 200 ms. Subjects were asked to press/release a button when the tone was audible/inaudible which resulted in decreasing/increasing the tone level in 6 (initial step) or 2 dB steps. Midpoints between reversals were calculated for each ascending run. The tracking procedure was considered to have converged to the subject's threshold if the standard error of the mean was less than 1 dB.

SOAE Recordings

Only ears with no detectable spontaneous activity near the probe frequency were included, reducing the possibility that PTC measurements were compromised by interactions between SOAE and external stimuli (e.g., beats, roughness, see Long 1998). Plausibly, SOAEs could also interact with SFOAE STC recordings, although data addressing that issue have not appeared in the literature.

SOAEs were measured in the absence of external stimulation using spectral averaging for ~2 min (sampling rate 32 kHz, buffer size 65,536 points) with Sysres software (Neely and Stevenson 2002). SOAE with levels at least 3 dB above the adjacent noise floor were identified. The recordings were repeated when obvious artifacts (e.g., due to subject movement) were detected.

SFOAE Recordings

Stimulus delivery and response measurement were controlled by Emav software (Neely and Liu 2011) for SFOAE "fine structure" recordings or by custom-made software for SFOAE input–output (IO) functions and STCs. For all measurements, SFOAE residuals were calculated as the difference between the averaged responses to the probe tone alone and to the probe tone in the presence of a suppressor tone; the resulting waveform was analyzed with a Fast Fourier transform (FFT) to obtain the SFOAE residual (Dreisbach et al. 1998). The residual measures the amount of SFOAE suppression by another tone. Two repetitions of the probe alone and probe plus suppressor time–domain averages were stored in separate buffers. The noise floor was estimated at the probe frequency from the spectrum of the difference between time–domain responses stored in the two buffers. Trials demonstrating high noise levels were repeated automatically if the noise exceeded a pre-defined criterion described below.

Tuning curves were obtained for each subject at nominal probe frequencies of 1,000 and 4,000 Hz. Because SFOAE amplitudes may vary rapidly with frequency (demonstrating so-called fine structure; Kemp and Chum 1980; Zweig and Shera 1995; Shera

and Guinan 1999), actual probe frequencies were selected as those evoking the highest SFOAE levels within ±100 Hz of 1,000 Hz and within ±200 Hz of 4,000 Hz (referred here as f_{probe}). Although behavioral thresholds may also demonstrate "fine structure" (e.g., Elliot 1958; Long 1984), we chose to optimize the test frequencies only *re.* SFOAE fine structure to ensure the best available SNR for STCs recordings. SFOAE fine structure was characterized with fine frequency steps from 811.7 to 1184.3 Hz (21.5 Hz steps) and from 3,682.2 to 4,285.1 Hz (43.1 Hz steps), with the probe level fixed at 20 and 30 dB SPL, respectively. The suppressor frequency was fixed at 43.1 Hz below the probe frequency at a level of 60 dB SPL. In such conditions, nearly complete or complete suppression is expected so that the measured SFOAE residual probably accurately represents the total SFOAE (Brass and Kemp 1993; Keefe et al. 2008). For each f_{probe}, the hearing threshold was measured (Table 1) and an SFOAE IO function was obtained for probe levels from 10 to 50 dB SPL (in 5 dB steps) using the same suppressor conditions as for the fine-structure recordings. The noise rejection criterion was typically set to −12 dB SPL.

The SFOAE STCs were measured as iso-residual curves for as many as three suppression (residual) criteria as a function of suppressor frequency for f_{probe} at levels of 10, 20, and 30 dB SL (Table 1). For each probe level and suppressor frequency, the suppressor level was varied automatically using a tracking procedure until the SFOAE residual was within ±1 dB of the residual criterion. The SFOAE STCs were measured for up to three residual criteria: −6, 0, and 6 dB SPL at each probe level (the available range of criteria was estimated based on the SFOAE IO function). The suppressor frequency (f_{sup}) was varied from $0.4f_{probe}$ to $2.1f_{probe}$ with a resolution of 5 points/octave and with increased resolution to 15 points/octave in the range from $0.9f_{probe}$ to $1.4f_{probe}$. The suppressor was never a harmonic or a subharmonic of the f_{probe}. Data collection was automatically terminated when the suppressor level reached 85 dB SPL, when no response meeting the threshold criterion was found in 15–20 attempts or when the noise level exceeded a predefined noise rejection criterion in 4 consecutive attempts. The noise rejection criterion was set at −12 dB SPL except for a few cases when it was raised to −10 dB SPL (but never for the −6 dB SPL criterion curves).

Psychophysical Tuning Curves

The PTCs were collected with a "fast" method (Sęk et al. 2005; Charaziak et al. 2012). The gated tonal probe, fixed in frequency, was presented simultaneously with a narrowband masker (200 or 320 Hz wide) for which the level was controlled by the subject via a button, as in Békésy audiometry, while the masker center frequency changed continuously in time from low to high (upward sweep) or from high to low (downward sweep). Subjects were instructed to press a button when the tonal probe was audible and to release the button when the tone became inaudible; the level of the noise was increased/decreased at fixed rate (4 dB/s) in 0.5 dB steps. The points at which the button was pressed or released were recorded, producing a tracking record of masker levels as they crossed just below/above the masked threshold for the probe as a function of the masker center frequency.

The fast PTC was implemented with custom written software (MATLAB, MathWorks) that generates and controls the signals via the arsc.dll library developed by Dr. Stephen Neely (ARSC API, 2010 see http://audres.org/). The pulsed probe was presented at fixed level of 10 dB SL at the frequency used for SFOAE STC recordings (Table 1). The probe was 500 ms in duration tone with 25 ms rise/fall times, presented with interstimulus intervals of 200 ms. The masker waveform was synthesized using MATLAB and stored on the hard drive (for details regarding signal synthesis see Sęk et al. 2005; Sęk et al. 2007; Sęk and Moore 2011). In brief, the 240-s masker waveform was synthesized by overlapping 7,500 short duration (~46 ms) segments of narrowband noise. The noise segments were generated in the frequency domain with a sampling rate of 44.1 kHz for 2,048 points and then transformed to the time domain

TABLE 1

Optimized probe frequencies from each individual's SFOAE fine structure and corresponding hearing thresholds

Subject ID/gender/ear	f_{probe} *(Hz)*	*Hearing threshold (dB SPL)*	f_{probe} *(Hz)*	*Hearing threshold (dB SPL)*
kc02ML	947	15	4,199	19
kc03FL	990	17	4,199	12
kc04FR	926	10	4,155	17
kc07ML	1098	6	4,005	10
kc12FL	990	10	4,005	13
kc13FR	968	8	4,112	13
kc15FR	947	7	4,026	6
kc18FL	968	6	4,026	14
kc20MR	990	6	3,940	18
kc21FL	1,076	12	3,983	12

with an inverse FFT. After gating with a Hanning window, the segments were overlapped in time by 50 % such that each subsequent segment had a higher/lower center frequency than the previous one for upward/downward sweep. As a result, the synthesized masker waveform was a narrowband noise with a center frequency that changed uniformly in time on a log frequency scale over the $0.5f_{probe}$–$2f_{probe}$ range. To minimize beat-detection cues, the masker bandwidth was set to 200 Hz for probe frequencies ~1,000 Hz and to 320 Hz for probe frequencies ~4,000 Hz (Kluk and Moore 2004; Sęk et al. 2005). The masker level never exceeded 90 dB SPL. To allow the subject to become familiar with the procedures, the starting masker level was always set below the probe level and the masker center frequency was held constant until 4 reversal points were obtained. The probe frequency/noise sweep direction conditions (4 in total) were presented in random order. The subjects were given a 10–15-min training prior to data collection.

Data Analysis

The tuning curves were characterized with several parameters to facilitate comparisons between PTCs and SFOAE STCs and to evaluate the effects of probe level and residual criterion on the features of SFOAE STCs. The tuning curve parameters were: frequency at the tuning curve tip (f_{tip}, tuning curve minimum), masker/suppressor level at the tip (L_{tip}), width measured 10 dB above the tuning curve tip (BW10), slopes of tuning curve sides (in dB/octave), and tip-to-tail ratio (in dB). The BW10 was calculated across the widest part of the curve (e.g., ignoring double tips or other irregularities). The tuning curve slopes were calculated for two ranges: low-frequency (LF) side slope ($-0.6 \leq f_{sup} \leq 0$ octaves re. f_{tip}) and high-frequency (HF) side slope ($f_{sup} \geq 0$ octaves re. f_{tip}) for curves having at least 3 data points in these ranges. The tip-to-tail ratio was calculated as the difference between L_{tip} and the masker/suppressor level at a frequency 0.6 octaves below f_{probe}. For each suppressor frequency, the phase of the SFOAE residual was recorded at the criterion threshold to gauge the SFOAE generation pattern. The SFOAE phases were unwrapped across f_{sup} to form an iso-response phase curve paired with each SFOAE STC.

The PTCs obtained with the fast method are jagged due to tracking above and below the masked threshold (Fig. 1, thin lines). Thus, raw PTC must be smoothed/modeled to extract the masker levels necessary to just mask the probe across the range of masker center frequencies. Charaziak et al. (2012) showed that the LOESS (local polynomial regression fitting) smoothing (Cleveland 1979, 1994) with the smoothing parameter set at 0.25 allows for good approximation of the PTC without

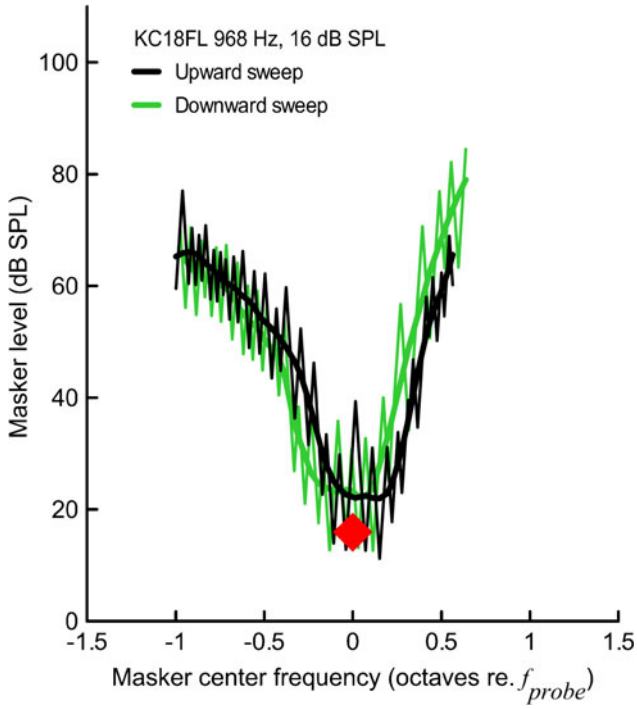

FIG. 1. PTCs collected with "fast" method for upward masker sweep (*black*) and downward masker sweep (*green*). The raw tracking data are shown with *thin lines*. To find the level of the masker required to just mask the probe, the raw data were smoothed with the LOESS algorithm with smoothing parameter α set at 0.25 (*bold lines*). The tonal probe parameters are indicated with a *red diamond*.

distorting the pattern in the data. Accordingly, all tuning curve parameters were calculated from LOESS-smoothed PTCs separately for an upward and a downward frequency-swept masker (see Fig. 1, bold lines for examples of smoothed PTCs), and then if not stated otherwise, averaged together for each subject to minimize the effects of masker sweep direction (Kluk and Moore 2006).

When SFOAE STC contained missing points or outliers, the data points were approximated with linear interpolation or re-measured if time allowed. To calculate average STCs across subjects, f_{sup} was transformed to octaves re. f_{probe}. Due to limited resolution of the SFOAE STC program (see Instrumentation) and differences in f_{probe} frequencies in different subjects, some STCs required resampling to allow averaging. The average suppressor threshold for a given suppressor frequency was calculated only if at least three data points were available. The iso-response phase curves were normalized to the phase value at the f_{sup} just below f_{probe} to minimize the effect of intersubject differences in absolute phase and then averaged with the same procedures as STCs.

Analogous procedures were applied to calculate average PTCs. The upward sweep and downward sweep LOESS-smoothed PTCs were averaged separately, and then normalized to the frequency at the tip to compensate for the horizontal shift resulting from

the masker sweep direction (Fig. 1) and finally averaged to obtain a mean curve.

The SFOAE IO functions were used to estimate the "total" SFOAE amplitude at the probe levels used for SFOAE STC recordings based on cubic-spline interpolation of the IO functions (Table 2).

All calculations were carried out in MATLAB. Statistical testing was performed with a general linear model adjusted for the correlations between repeated measures within a subject, if not stated otherwise. The model included up to two-way interactions, if available. Post hoc analyses were performed with Bonferroni's method. Statistical testing was conducted in SPSS (SPSS Inc., Chicago).

RESULTS

SFOAE Suppression Tuning Curves

General Observations—Suppression Thresholds. We collected 76 SFOAE STCs for f_{probe} at 1,000 Hz and 66 SFOAE STCs for f_{probe} at 4,000 Hz (excluding retest data). Mean SFOAE STCs are shown in Fig. 2. Due to the limited suppression range in some subjects, it was not possible to record STCs for all conditions (also see Table 2). Overall, STCs near the suppression onset (residual criterion of −6 dB SPL) could be recorded for all but two subjects that had high noise floors for the 30 dB SL probe level. Perplexing physiological "on-band" noise that increases in level with increasing probe level has been reported for SFOAEs (Schairer et al. 2003; Schairer and Keefe 2005). This noise appears to have been especially high in these subjects. For other subjects and conditions, the average noise floor was −19.7 dB SPL (SD=6.0 dB).

The average SFOAE STCs were usually "V-shaped" as observed for behavioral tuning. However, for the 1,000-Hz STCs, there was a change from an irregular-shaped (e.g., "double-tipped") curve with shallow high-frequency slope to a "V-shaped" curve with a steep high-frequency slope when increasing the residual criterion from −6 to 6 dB SPL for a 30-dB SL probe (see the right-hand column in Fig. 2) or when decreasing the probe level from 30 dB SL to 10 dB SL for a residual criterion of −6 dB SPL (see the bottom row in Fig. 2). On the other hand, the 4,000-Hz, STCs were uniform in shape and less affected by measurement conditions with the exception of STCs at 30 dB SL/6 dB SPL which demonstrated a blunt tip. In most cases, the 4,000-Hz STCs were more narrow (on logarithmic frequency scale) and demonstrated more pronounced transitions between tip and tail on the low-frequency side as compared to the 1,000-Hz STCs. For all conditions, larger intersubject variability in suppression threshold was observed on the high-frequency side of the curve as compared to the low-frequency side (see error bars in Fig. 2).

In the individual data, it was common to observe double-tipped STCs or irregular-shaped STCs with multiple inflections, especially for the higher probe levels and/or lower residual criteria for the 1,000-Hz probe (Fig. 3A–C). It is noteworthy that despite a clear transition in the mean data toward a uniformly shaped STC with increasing criterion or decreasing probe level (Fig. 2, black), the effects of recording conditions on STC shapes were not consistent across subjects. For instance, increasing the residual criterion for a fixed probe level could result in either total or partial reduction of the depth of the second tip (Fig. 3C), but in some cases no appreciable change in STC shape around the tip was observed. In contrast, individual 4,000 Hz STCs were usually uniform in shape across all recording conditions (Fig. 3D–F) just as observed for the mean data (Fig. 2, gray).

SFOAE Residual Phase at Suppression Threshold. Mean phases of the SFOAE residual at the criterion threshold are shown in Fig. 4. The mean phase did not vary by more than ±0.25 cycles with f_{sup}. In general, the phase curves demonstrated more intersubject variation and were more affected by changes in the recording conditions for the 1,000-Hz probe as compared to the 4,000-Hz probe, which agrees with the trend observed for suppression threshold curves (Fig. 2). For the 1,000-Hz probe, there was increased phase variability with increasing f_{sup}, particularly for the 30 dB SL/−6 dB SPL criterion

TABLE 2

Mean total SFOAE estimates (SD) at optimized probe frequencies (Table 1) for probe levels of 10, 20, and 30 dB SL derived from IO functions

f_{probe} (Hz)	Mean hearing threshold at f_{probe} (dB SPL)	Probe level (dB SL)	Mean total SFOAE (dB SPL)	Range of total SFOAE (dB SPL)
1,000	9.7 (3.9)	10	−0.9 (3.7)	−6.5 to 7.0
		20	6.0 (3.3)	0.8 to 13.3
		30	10.5 (3.7)	4.9 to 19.2
4,000	13.4 (3.9)	10	−2.4 (3.4)	−7.2 to 2.1
		20	4.2 (3.4)	−2.3 to 8.0
		30	8.3 (3.4)	1.8 to 12.7

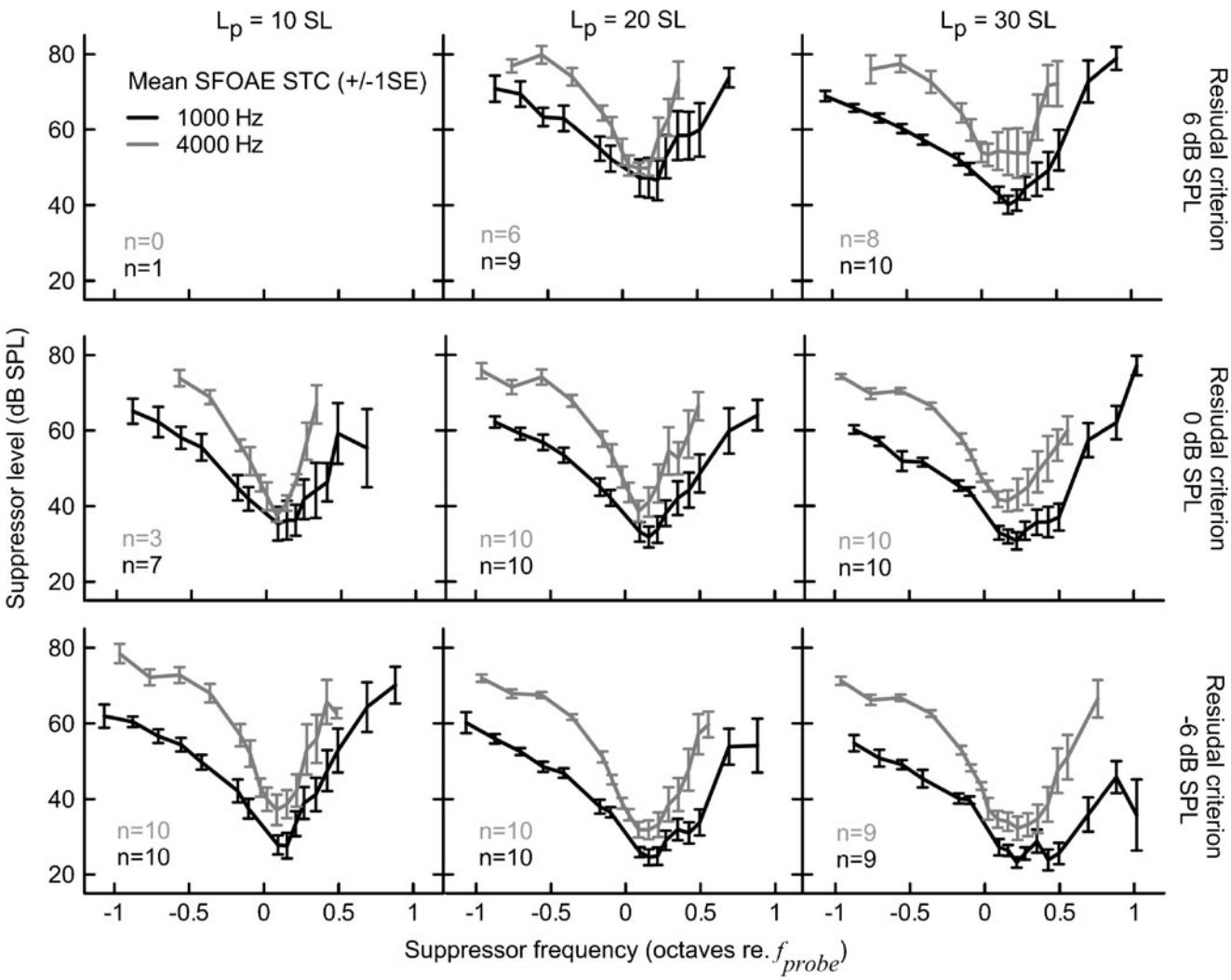

FIG. 2. Mean SFOAE STC at 1,000 (*black*) and 4,000 Hz (*gray*) probe frequencies for 10, 20, and 30 dB SL probe levels (*columns*) and −6, 0, and 6 dB SPL residual criteria (*rows*). *Error bars* denote ±1 standard error (SE). The number (*n*) of STCs collected for each condition is indicated in each subplot.

condition (Fig. 4). This increased variability could be due to the increased noise level at higher probe levels; yet, the level of the noise floor at the probe frequency was not suppressor-frequency dependent (data not shown), which argues against such an explanation.

Although the mean residual phase curves remained relatively independent of f_{sup} across recording conditions, individual data suggest that phase behavior consistently changed *within* a given subject. The overall pattern of phase shifts differed across subjects and thus it was cancelled out when averaged. For instance, for subject KC15FR at f_{probe} of 947 Hz and 30 dB SL, there was a clear phase shift at $f_{sup} > f_{probe}$ that progressively decreased with decreasing probe level (Fig. 5C to A, black lines) and with increasing residual criterion (Fig. 5C, compare the black and light gray lines). To emphasize the high test–retest repeatability of the phase behavior within a given subject, data for the condition most susceptible to noise (30 dB SL/−6 dB SPL) collected during a retest session are shown in Fig. 6A. A similar trend, albeit on a much smaller scale, was observed for the 4,000-Hz phase curves (Fig. 5D–F); for this f_{probe} only one example of a doubled-tipped STC, accompanied by relatively large phase shifts, was observed (see Fig. 6B). The pattern of phase shifts was preserved for STCs measured with f_{sup} chosen with reduced frequency spacing (25 points/octave, Fig. 6, red lines) indicating that the inconsistency in phase behavior across subjects was not due to errors in phase unwrapping.

We investigated the effects of recording conditions on phase by calculating the standard deviation of the mean unwrapped phase value for a given curve (Fig. 7). Across subjects there was a common trend of decreasing variability of the residual phase with increasing criterion

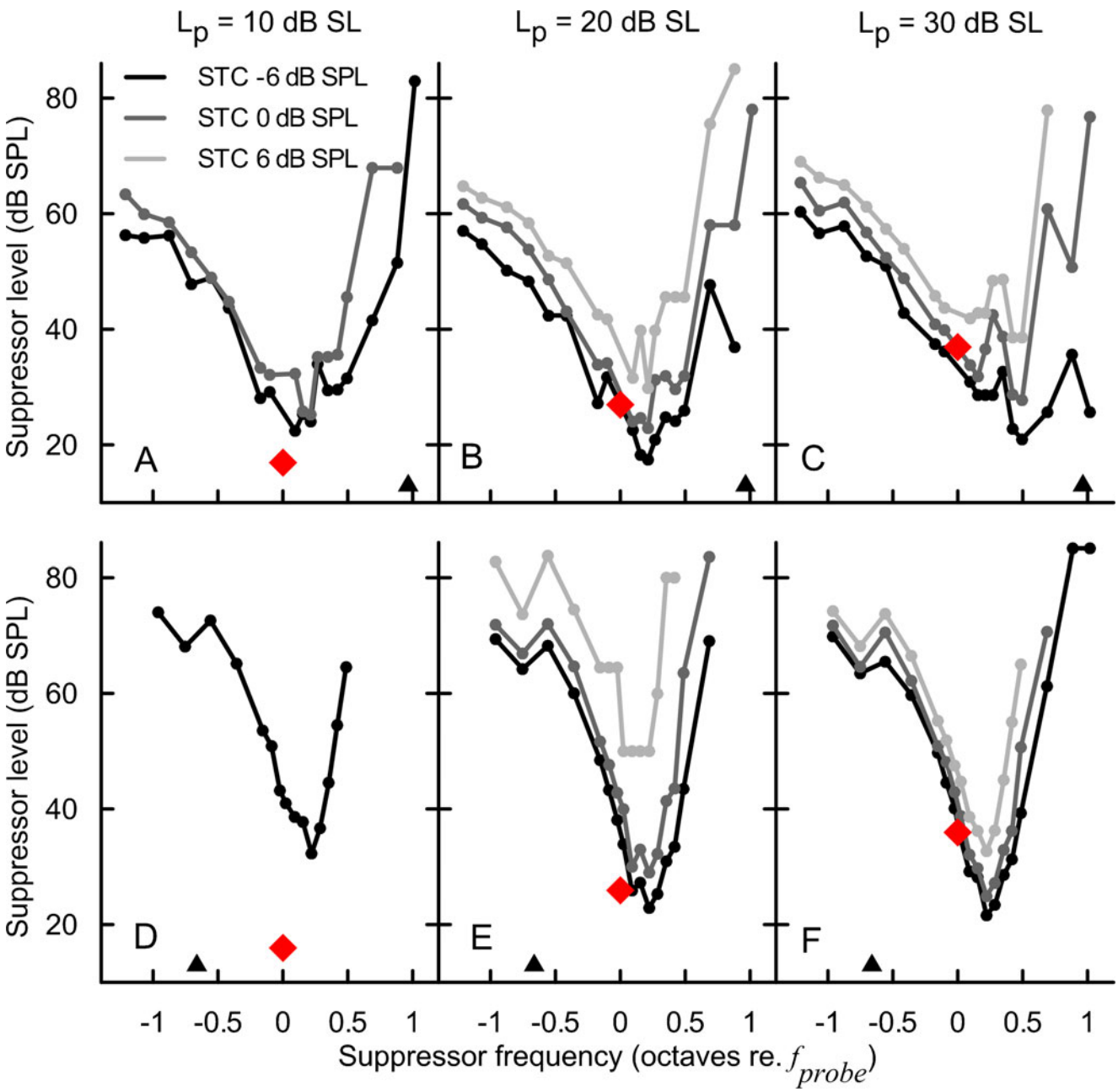

FIG. 3. SFOAE STCs for subject KC15FR at the 947 Hz (**A**–**C**) and the 4026 Hz probe frequency (**D**–**F**). The data are grouped in columns according to the probe level (10, 20, and 30 dB SL), and the *line color* indicates the SFOAE residual criterion: −6 (*black*), 0 (*dark gray*), and 6 dB SPL (*light gray*). The *red diamonds* denote the probe parameters. The *triangles* indicate the frequency of the SOAEs.

($F_{2,33.9}$=16.2, p<0.001 for 1,000 Hz; $F_{2,27.8}$=24.4, p<0.001 for 4,000 Hz) and decreasing probe level ($F_{2,26.6}$=10.0, p<0.001 for 1,000 Hz; $F_{2,22.1}$=15.3, p<0.001 for 4,000 Hz). For the 1,000-Hz probe, there was a significant interaction between the probe level and the residual criterion ($F_{4,22}$=3.3, p=0.03), indicating that the criterion had its largest effect on the phase variability at higher probe levels. No significant interaction was found for the 4,000-Hz probe. Although the main effects of recording conditions on phase variability were significant for both probe frequencies, it is clear that the magnitude of change was much smaller for 4,000 Hz (note the *Y* axis scale difference between panels A and B of Fig. 7).

SFOAE STC Parameters—The Effects of Residual Criterion and Probe Level. The tip of the STC (f_{tip}) was shifted above the probe frequency in 97 % of curves. The size of the shift in f_{tip} tended to increase together with increasing the probe level and decreasing the residual criterion (Fig. 8A, B). The ANOVA analyses showed a significant effect of the probe level on the f_{tip} shift ($F_{2,29.6}$=6.6, p=0.004 and $F_{2,26}$=3.8, p=0.036 for 1,000 and 4,000 Hz, respectively); however, the

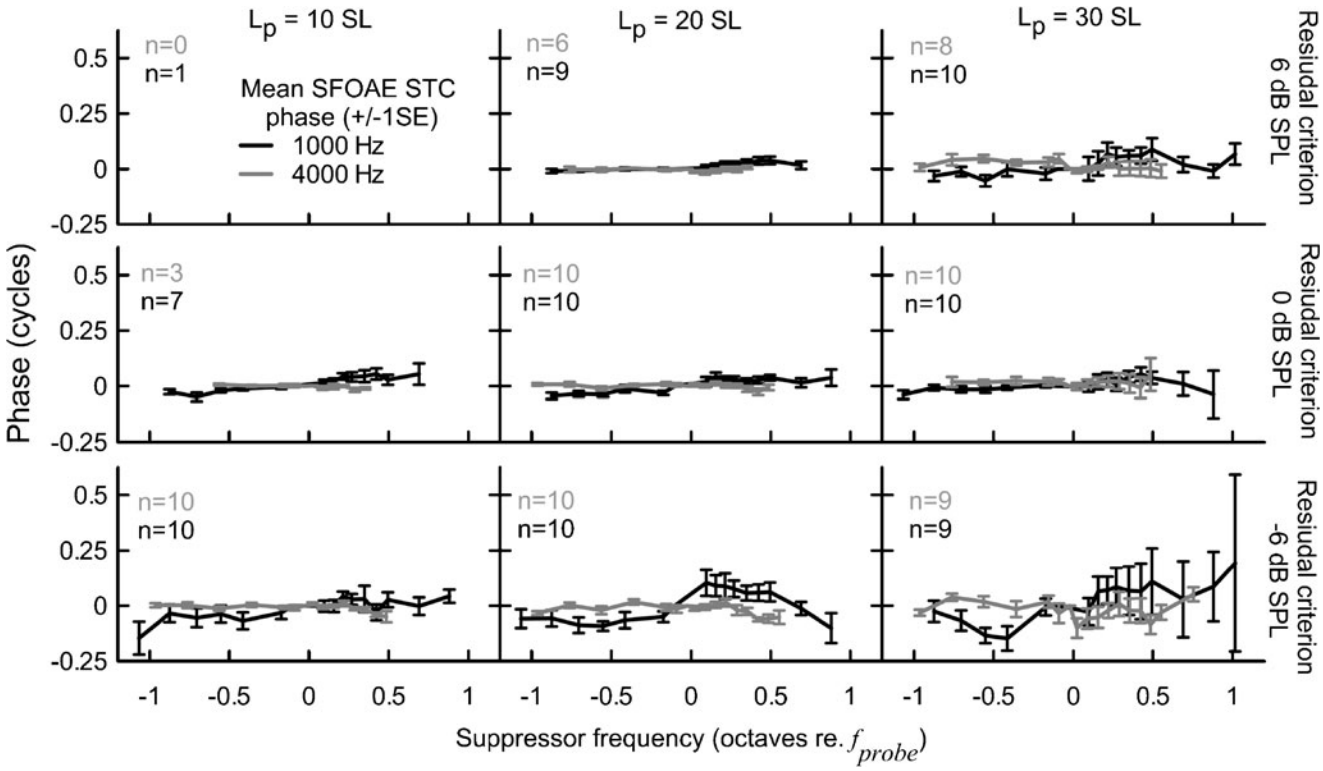

FIG. 4. Mean phase of the SFOAE residual at the criterion threshold. Other plot conventions are as in Fig. 2.

effects of residual criterion did not reach significance ($F_{2,32.9}$=1.8, p=0.19 and $F_{2,22.2}$=3.3, p=0.06 for 1,000 and 4,000 Hz, respectively), likely due to insufficient power of the sample size. No significant interactions between the criterion and probe level were found. A stronger effect of the probe level was observed for the 1,000-Hz STCs where all pairwise comparisons showed a clear trend for the tip of the curve shifting toward the f_{probe} with decreasing probe level (p<0.05). For the 4,000-Hz STCs, there were no significant differences in f_{tip} between the lowest two probe levels, but they were significant for other level comparisons (p<0.05).

Increasing the residual criterion (i.e., toward full suppression) led to shifting the whole STC upwards

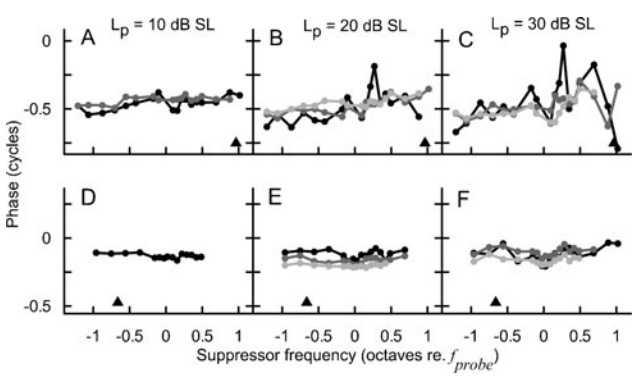

FIG. 5. The SFOAE residual phase curves at the criterion threshold for the STCs shown in Fig. 3. Plotting conventions as in Fig 3.

(Figs. 2, 3, and 8C, D). For both probe frequencies, there were significant main effects of the probe level (p<0.02) and residual criterion (p<0.001) on the suppressor level at the tip (in dB SL), with no significant interactions. *Post hoc* analyses revealed that increasing the residual criterion led to an upward shift in L_{tip} (p<0.001). The effect of increasing the probe level was less pronounced; a significant downward shift in L_{tip} was observed for the 1,000-Hz STCs when the probe level was increased from 20 to 30 dB SL and from 10 to 20 dB SL, p<0.05.

The width of SFOAE STCs (expressed as BW10) did not change significantly with increasing probe level for either probe frequency ($F_{2,25.9}$=2.0, p=0.16 and $F_{2,28.9}$=0.60, p=0.55 for 1,000 and 4,000 Hz, respectively, Fig. 9). The ANOVA analyses showed a significant main effect of the residual criterion on the BW10s of the 4,000-Hz STCs ($F_{2,27.6}$=3.4, p=0.048) indicating that increasing the residual criterion led to a sharper estimate of tuning (Fig. 9B); yet none of the pairwise comparisons were significant (p>0.9). There was no main effect of the criterion on width of the 1,000-Hz STCs ($F_{2,30.3}$=0.73, p=0.49), and no significant interactions between the probe level and criterion for either probe frequency (p>0.4).

The LF slopes did not change significantly with either the residual criterion or probe level for both probe frequencies, and no interactions were observed (p>0.17). Mean LF slopes across all conditions were –41 dB/oct

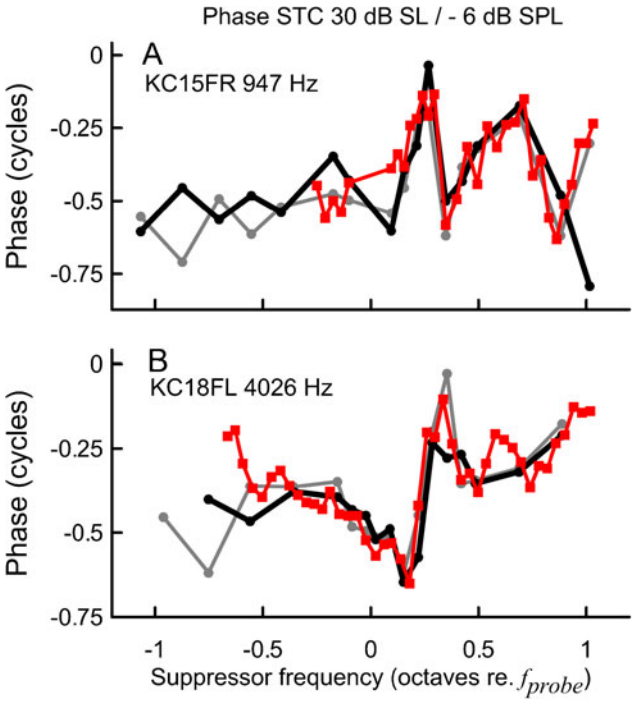

FIG. 6. SFOAE STC residual phase for subjects KC15FR at 947 Hz (**A**) and KC18FL at 4,026 Hz (**B**). The probe level was fixed at 30 dB SL and the residual criterion at −6 dB SPL. The *black* and *gray solid lines* correspond to recordings made with resolution of 15 points/octave around the tip and 5 points/octave at the flanks (see the "Materials and Methods" section for details), and the *red lines* correspond to recordings made with a resolution of 25 points/octave. Data plotted in *gray* and *red* were collected during a retest session (5–8 weeks later).

(SD=20 dB/oct) and −60 dB/oct (SD=18 dB/oct) for 1,000 and 4000 Hz, respectively. The high-frequency slopes became steeper with increasing the residual criterion ($F_{2,37}$=3.8, p=0.032 and $F_{2,23}$=5.2, p=0.014 for 1,000 and 4,000 Hz, respectively). Multiple comparisons showed that at 1,000 Hz the HF slopes changed by an average of 27 dB/oct when increasing the residual criterion from −6 to 6 dB SPL (p<0.05). An analogous change was observed at 4,000 Hz (24 dB/oct), but it did not reach significance (p=0.13). There were no main effects of the probe level on the HF slopes and no significant interactions. In general, the mean HF slopes ranged from 41 to 92 dB/oct for 1,000 Hz and from 94 to 137 dB/oct for 4,000 Hz across the conditions. For both probe frequencies, the HF slopes were significantly steeper than the LF slopes (expressed as their absolute values, $F_{1,9.1}$=19.3, p=0.002 and $F_{1,9.3}$=71.2, p<0.001 for 1,000 and 4,000 Hz, respectively), which reflects the asymmetrical tuning curve shape (e.g., see Fig. 2).

The tip-to-tail ratio decreased with increasing residual criterion ($F_{2,23.7}$=4.9, p=0.016 and $F_{2,23.4}$=7.2, p=0.004 for 1,000 and 4,000 Hz, respectively). On average, the tip-to-tail ratio decreased by 5.8 dB (p<0.001) for 1,000 Hz and by 2.9 dB for 4,000 Hz (p<0.05) when increasing the criterion from −6 to 6 dB SPL. No differences were observed between the −6 and 0 dB SPL curves. The effect of the probe level was significant only for the 4,000-Hz probe ($F_{2,26.0}$=5.6, p=0.009; for 1,000 Hz, $F_{2,21.2}$=0.094, p=0.91). Multiple comparisons showed that the tip-to-tail ratio for 10 dB SL curves was larger than either 20 (by 4.1 dB) or 30 dB SL (by 5.6 dB) STCs (p<0.001). No interactions were found for either probe frequency. The mean tip-to-tail ratios varied across the recording conditions from 17.6 to 27.4 dB for the 1,000-Hz STCs and from 25.2 to 32.8 dB for the 4,000-Hz STCs.

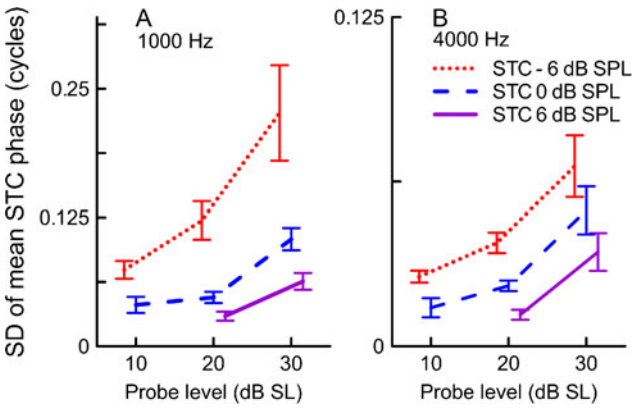

FIG. 7. Variation in the SFOAE residual phase at criterion threshold expressed as the standard deviation of the mean unwrapped phase across suppressor frequencies for the 1,000 Hz STCs (**A**) and the 4,000 Hz STCs (**B**) as a function of the probe level. Mean values and SE are shown. *Red dotted line* for STCs collected for the −6 dB SPL criterion, *blue dashed line* for the 0 dB SPL criterion, and *purple solid line* for the 6 dB SPL criterion. Note the *Y* axis scale difference for **A** and **B**. Note that probe levels in Figs.7–9 have been offset slightly for clarity.

Psychophysical Tuning Curves

Masker Sweep Direction. As previously reported (Sęk et al. 2005), the masker sweep direction had a significant effect on the frequency of the PTC tip ($F_{1,8}$=10.4, p=0.012 and $F_{1,9}$=47.6, p<0.001 for 1,000 and 4,000 Hz, respectively; see Fig. 1 for an example). The f_{tip} was shifted toward higher frequencies (mean shift 0.041 and 0.052 octaves re. f_{probe} for 1,000 and 4,000 Hz, respectively) for upward masker sweeps and toward lower frequencies (mean shift −0.035 and −0.023 octaves re. f_{probe} for 1,000 and 4,000 Hz, respectively) for downward masker sweeps. The L_{tip}s, BW10s, HF and LF slopes, and tip-to-tail ratio were not affected by the direction of the masker sweep for either the 1,000 or 4,000 Hz curves (p>0.1). Thus, the masker sweep direction affected only the horizontal position of the curve, but not its other parameters. The PTC parameters were averaged across upward and downward sweep directions (Kluk and Moore 2006) for the subsequent analyses (except for subject KC13FR, for whom only 1,000 Hz upward sweep data were available).

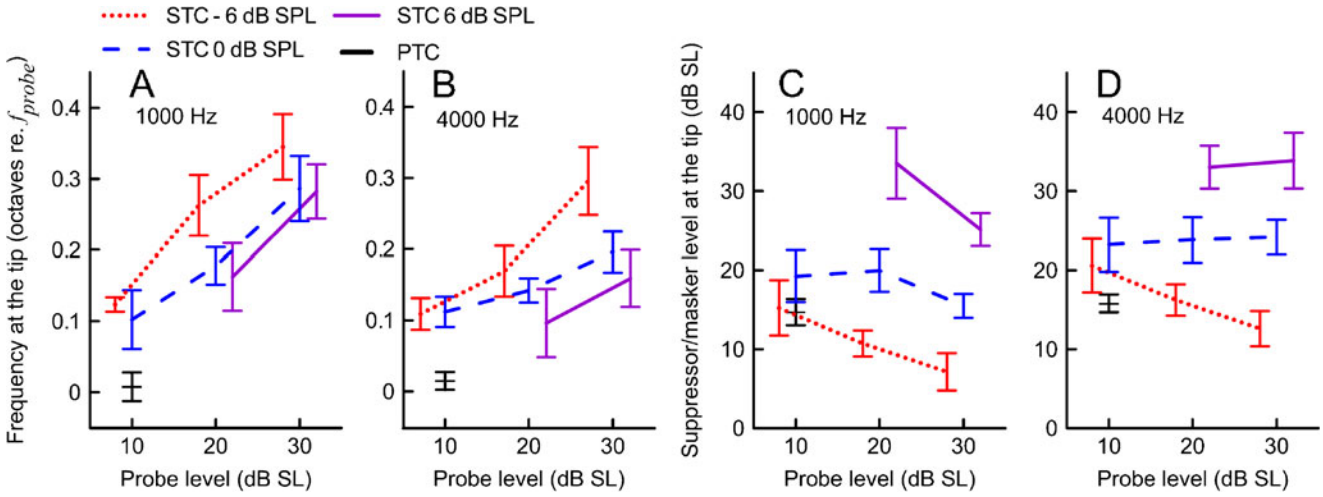

FIG. 8. Mean suppressor frequencies and suppressor levels at the tip of SFOAE STCs at 1,000 (**A** and **C**) and 4,000 Hz (**B** and **D**) as a function of probe level. The mean data for PTCs are shown in *black*. *Error bars* denote ±1SE. Other plotting conventions as in Fig. 7.

PTC Parameters. After accounting for the effect of masker sweep direction, the average f_{tip}s closely coincided with the probe frequency (Fig. 8A, B, black). The L_{tip} was consistently higher than the probe level (10 dB SL) for both probe frequencies (Fig. 8C, D, black). The 4,000-Hz PTCs were wider on a linear frequency scale than the 1,000-Hz curves (Fig. 9A, B, black) as previously reported (e.g., Moore 1978). The mean HF slopes were 89 dB/oct (SD=17 dB/oct) and 121 dB/oct (SD=25 dB/oct) for the 1,000 and 4,000-Hz PTCs, respectively. Similarly, the mean LF slopes were −62 dB/oct (SD=10 dB/oct) and −71 dB/oct (SD=8 dB/oct). For both probe frequencies, HF slopes were significantly steeper than LF slopes ($F_{1,9}$=26.8, p=0.001 and $F_{1,9}$=45.7, p<0.001 for 1,000 and 4,000 Hz, respectively). Mean tip-to-tail ratios were 33.8 (SD=5.1 dB) and 40.1 dB (SD=3.4 dB) for the 1,000 and 4,000-Hz PTCs, respectively.

Relation Between Sharpness of Tuning of SFOAE STC and PTC

To evaluate the potential of SFOAE STCs for estimating behavioral tuning, we compared the widths of PTCs and STCs collected in the same group of subjects. We expected SFOAE STCs and PTCs to have similar widths (BW10) when the 10 dB SL probe level was used. Recording SFOAE STCs at higher probe levels has the advantage of stronger emissions (better SNR); however, increasing the probe level may result in SFOAE STCs overestimating the sharpness of behavioral tuning measured with low probe levels, particularly for low SFOAE residual criteria (Kemp and Chum 1980).

Mean BW10 values were similar for the STCs and PTCs when evaluated at the same probe levels (10 dB SL, Fig. 9). At higher probe levels, the 4,000-Hz STCs tended to be broader than PTCs, particularly for the lower residual criteria. This trend was not apparent for the 1,000-Hz STCs. To evaluate how well the widths of SFOAE STCs and PTCs correspond in an individual, we normalized the STC BW10 by the PTC BW10 for a given subject (referred here as the BW10 ratio). Although the mean BW10 ratios were close to 1 for most conditions (data not shown, trends can be inferred from Fig. 9), we observed considerable data scatter, with individual ratios ranging from 0.18 to 4.23 for 1,000 Hz and from 0.39 to 2.88 for 4,000 Hz. Examples of fits between individual SFOAE STCs (10 dB SL/−6 dB SPL) and PTCs are shown in Fig. 10. Even though STCs were recorded for the same conditions in these subjects, we observed a large variability in the degree of agreement between STC and PTC, as demonstrated by BW10 ratios listed

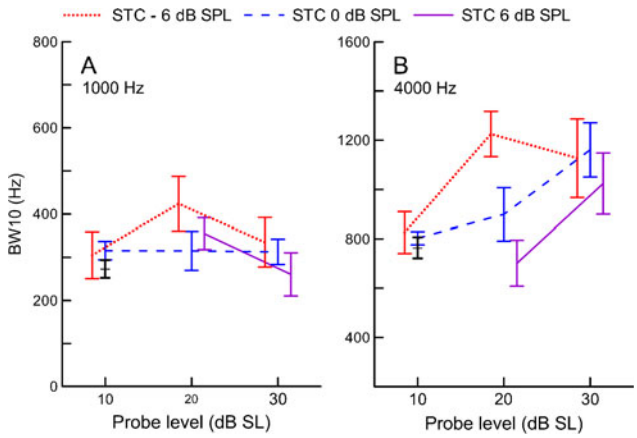

FIG. 9. Mean widths of SFOAE STCs at 1,000 (**A**) and 4,000 Hz (**B**) expressed as bandwidth 10 dB above tuning curve tip (BW10) as a function of probe level. The mean data for PTCs are shown in *black*. *Error bars* denote ±1SE. Other plotting conventions as in Fig. 6.

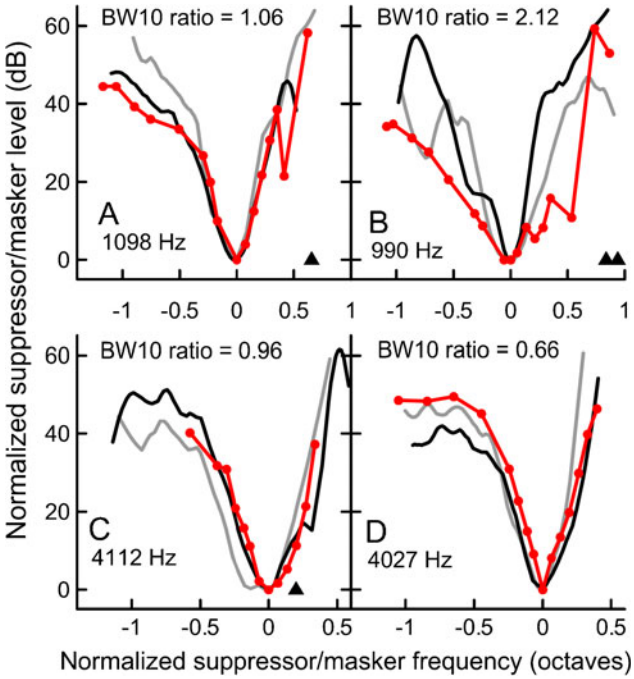

FIG. 10. Examples of individual SFOAE STC (in *red, circles*) and PTC (*black*—upward masker sweep; *gray*—downward sweep) fits for 1,000 (**A** and **B**) and 4,000 Hz (**C** and **D**). The *left panels* show examples of fits with BW10 ratios close to 1 ("good" agreement in terms of sharpness of tuning), whereas the *right panels* show examples of relatively poor agreement. All STCs were collected for 10 dB SL/−6 dB SPL condition. For this condition, the BW10 ratios ranged from 0.33 to 2.12 for 1,000 Hz data and from 0.66 to 1.62 for 4,000 Hz data. *Triangles* denote frequencies of SOAEs, if present.

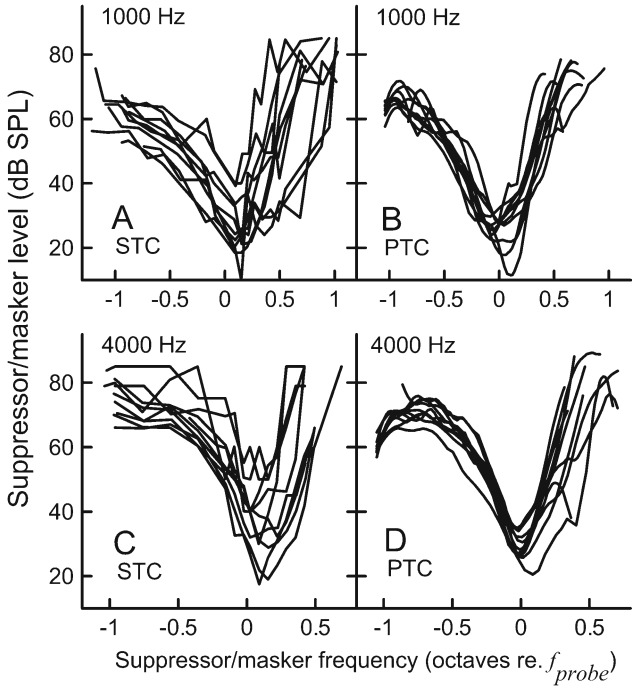

FIG. 11. Individual SFOAE STCs (10 dB SL/−6 dB SPL criterion condition) and LOESS-smoothened PTCs (upward sweep) for the 1,000-Hz probe (**A** and **B**) and the 4,000-Hz probe (**C** and **D**).

above each panel. Thus estimates of tuning measured with PTCs in individual subjects are not predicted reliably from the SFOAE STCs. Individual curves are plotted in Fig. 11 to illustrate the difference in variability of SFOAE STC and PTC shapes. Smoothing SFOAE STCs with the LOESS algorithm, as was done for PTCs, had a negligible effect on the observed irregularities, indicating that differences between the shapes of SFOAE STCs and PTCs were not due to smoothing. It is unlikely that the irregularity of the SFOAE STCs was due to the influence of noise because the test–retest repeatability for both PTCs and SFOAE STCs was very similar (see next section). Thus, the irregular shapes of STCs are most likely related to the SFOAE generation processes (see the "DISCUSSION" section).

When averaged across subjects, the SFOAE STCs and PTCs had similar widths, suggesting that behavioral and SFOAE-based estimates of tuning are related at the group level (Fig. 12). In general, the BW10 ratios for average curves were close to 1 for most of the residual criteria conditions when the probe level was either 10 or 20 dB SL (Table in Fig. 12). For the 20-dB SL probe, the −6-dB SPL criterion curves indicated broader tuning than PTCs, as expected. Surprisingly, increasing the criterion for 10 dB SL STCs resulted in increased BW10 ratios at 1,000 Hz. For 30 dB SL probe levels, all ratios exceeded unity.

Although the BW10 is a standard metric of the width of tuning curves, and therefore, a metric of frequency selectivity, comparing BW10s does not assess the agreement between overall shapes of tuning curves. As a measure of the accuracy with which the mean SFOAE STCs replicated the shape of the mean PTCs, we calculated mean absolute errors (MAE, Table 3). The average PTCs were interpolated with data points for which points were available for STCs. Curves were normalized to the tip frequency and the mean absolute difference between suppressor and masker levels at threshold was calculated across suppressor/masker frequencies. When considering only conditions for which SFOAE STCs were recordable for all subjects (n=10), the smallest MAEs were obtained for both probe frequencies for probe levels of 10 dB SL and a residual criterion of −6 dB SPL. Increasing the probe level to 20 dB SL was associated with an increase of MAEs, but the agreement was still reasonably good.

Test–Retest Repeatability

Two subjects (KC18FL and KC15FL) were retested after 5–8 weeks (in total, 8 PTCs and 29 SFOAE STCs were collected during retest sessions). To measure the test–retest repeatability, we used the MAE calculated

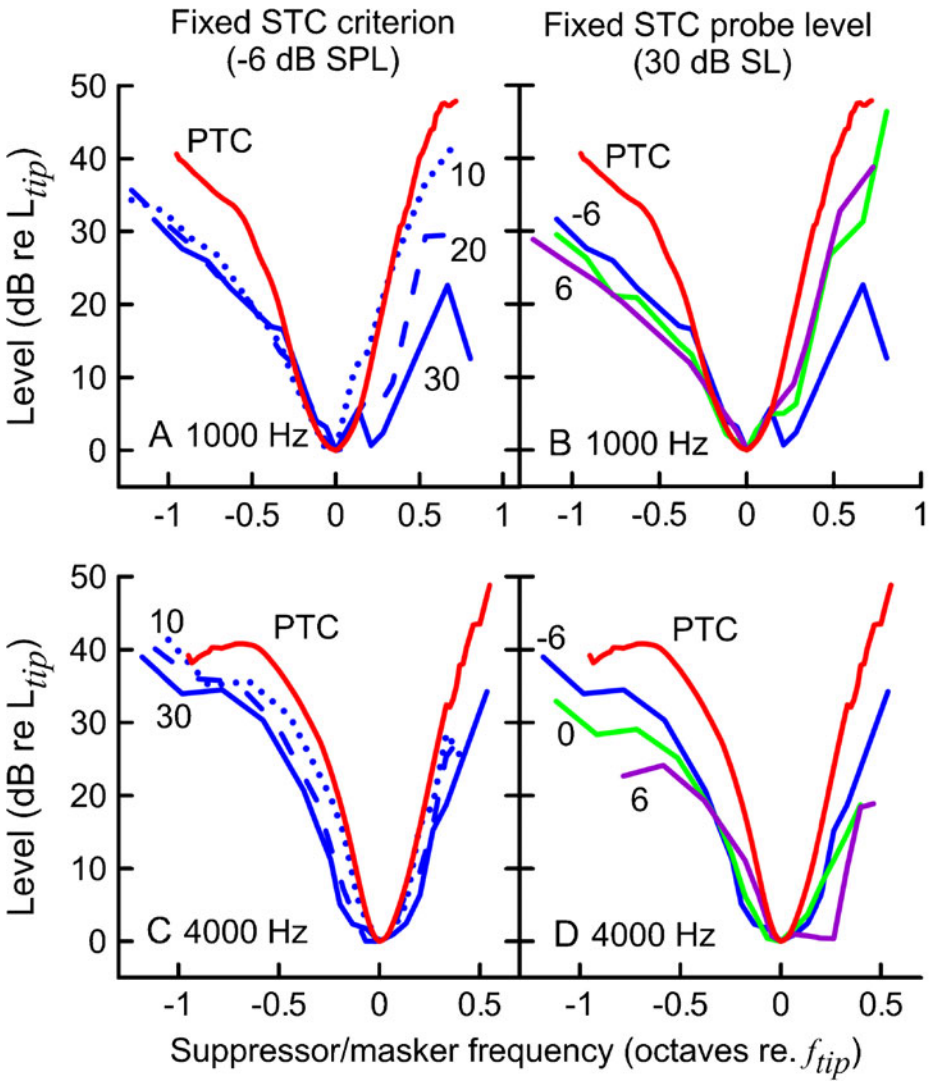

1000 Hz BW10 ratio

	10	20	30
-6	0.91	1.59	1.95
0	1.53	1.15	1.65
6	n.a.	1.33	1.49

4000 Hz BW10 ratio

	10	20	30
-6	1.12	1.59	1.96
0	0.94	1.01	1.80
6	n.a.	1.17	1.87

FIG. 12. Average SFOAE STCs (replotted from Fig. 2) and average PTCs for n=10 (*red*) for 1,000 (**A** and **B**) and 4,000 Hz (**B** and **C**) probe tones. In panels **A** and **C**, average STCs (in *blue*) for a fixed residual criterion (−6 dB SPL) and increasing probe level (10 dB SL—*dotted lines*, 20 dB SL—*dashed lines*, 30 dB SL—*solid lines*) are shown. In panels **B** and **D**, average STCs for a fixed probe level (30 dB SL) and changing criteria (−6 dB SPL—*blue*, 0 dB SPL—*green*, 6 dB SPL—*purple*) are shown. The tuning curves were normalized to their tip. The table on the left shows ratios of average STC BW10 to corresponding average PTC BW10 across STCs probe levels (*columns*) and criteria (*rows*). Note: BW10 ratios were calculated for average curves built for subjects that completed both conditions (for simplicity, average PTC for n=10 is only shown). The grayed BW10 ratios are for the curves plotted in panels **A**–**D**.

as the absolute difference of the first tuning curve relative to the second (a retest) for a given recording condition averaged over all f_{sup} common to both STCs. The MAE ranged from 0.79 to 15.6 dB for suppressor levels at the criterion threshold (grand average, 3.6 dB; SD, 2.8 dB; note: with the exception of one pair of STCs the MAE values did not exceeded 8 dB) and from 0.011 cycles to 0.1 cycles for the residual phases (grand average, 0.047 cycles; SD, 0.026). The 4,000-Hz STCs tended to have smaller MAEs (grand average, 2.2 dB; SD, 1.1 dB) than for the 1,000-Hz STCs (5.0 dB; 3.3 dB). MAEs for SFOAE residual phases were similar for the 1,000-STCs and the 4,000-Hz STCs (compare 0.041 cycles, SD 0.022 for 4,000 Hz and 0.052 cycles, SD 0.029 for 1,000 Hz).

Analogous calculations were performed for PTCs. The MAE varied from 1.9 to 3.3 dB with a grand average of 2.7 dB (SD 2.2 dB) with no indication of better test–retest repeatability for either probe frequency. Thus, PTCs and SFOAE STCs were similarly repeatable.

For comparison to the SFOAE STC test–rest data of Keefe et al. (2008), the mean of the difference of the first STC relative to the second STC was calculated for each recording condition and each subject, averaging over all f_{sup} in common for both STCs. The mean difference in suppression thresholds varied from –15.6 to 6.5 dB across the conditions, with a grand average

TABLE 3

Mean absolute errors (MAE) for average SFOAE STCs and corresponding average PTCs

		MAE (dB)		
f_{probe} (Hz)		10	20	30
1,000	−6	3.7 (10)	5.2 (10)	7.8 (9)
	0	8.8 (7)	4.8 (10)	6.6 (10)
	6	n.a.	9.9 (9)	8.1 (10)
4,000	−6	3.3 (10)	5.6 (10)	7.6 (9)
	0	2.5 (3)	4.6 (10)	8.9 (10)
	6	n.a.	4.9 (6)	11.3 (8)

Columns show data for STCs recorded at probe levels ranging from 10 to 30 dB SL; rows show data for STCs recorded for criteria ranging from −6 to 6 dB SPL. In parentheses, the number of subjects contributing to the average curve is shown

of −0.8 dB, which compares well with the 0.6 dB value reported by Keefe et al. (2008).

DISCUSSION

Stimulus-frequency otoacoustic emission suppression patterns have potential for estimating frequency selectivity of the auditory system (Kemp and Chum 1980; Keefe et al. 2008). So far, SFOAEs have gained little attention in the literature compared to other types of otoacoustic emissions, mostly due to technical difficulties with separating the response from the stimulus, which occur at the same frequency. Here, we follow-up on Kemp and Chum's (1980) observation made for one subject that SFOAE STCs can be as sharply tuned as behavioral tuning curves. We report SFOAE STCs and PTCs measured in 10 normally hearing ears, and we evaluate the effects of recording conditions (residual criterion and probe level) on SFOAE STC features.

Tuning Curve Parameters—Level and Frequency at the Tip

The mean masker level at the tip of the PTCs was similar to the mean suppressor level at the tip of the SFOAE STCs for smaller residual criteria and lower probe levels (Fig. 8C, D). For these conditions, comparisons of tuning derived from STCs and PTCs were probably not affected by differences in probe level (Eustaquio-Martin and Lopez-Poveda 2011). As observed by others, increasing the criterion toward full-suppression led to shifting the STC to higher levels (Figs. 2, 3, and 8C, D; see also Kemp and Chum 1980; Kemp et al. 1990; Brass and Kemp 1993; Kummer et al. 1995; Keefe et al. 2008). Increasing the probe level usually caused the curve to shift downward in level as also observed for compound action potential tuning curves constructed for a fixed residual criterion (Salt and Garcia 1990; Al'tman and Nikitin 2000).

The upward shift of the flanks of SFOAE STCs with increasing residual criterion at a fixed probe SL depended on the suppressor frequency, with smaller shifts observed for $f_{sup}<f_{probe}$ and larger shifts for $f_{sup}>f_{probe}$ (Fig. 3). This is consistent with reported shallower slopes of SFOAE suppression input–output functions obtained for $f_{sup}>f_{probe}$ than for $f_{sup}<f_{probe}$ (Brass and Kemp 1993; Keefe et al. 2008) as also observed for other types of OAEs (e.g., Zwicker and Wesel 1990; Long et al. 1991; Gorga et al. 2002). Likewise, a similar trend has been demonstrated in measures of two-tone suppression at the level of the basilar membrane (e.g., Ruggero et al. 1992; Cooper 1996) or single auditory nerve fibers (Delgutte 1990a). However, caution is needed to interpret such comparisons because these measures represent the response from a single localized region of the cochlea which is not likely to be true for OAEs (Guinan 1990; Brass and Kemp 1993; Siegel et al. 2005; Choi et al. 2008; Martin et al. 2010).

SFOAE STCs were consistently tuned to a frequency higher than the probe frequency in agreement with previous observations (e.g., Wilson 1980; Zurek 1981; Schloth and Zwicker 1983; Bargones and Burns 1988; Brass and Kemp 1993; Kummer et al. 1995; Zettner and Folsom 2003; Keefe et al. 2008). At the lowest probe levels, the tip of the SFOAE STCs was usually shifted above the probe frequency by an average of 0.09–0.12 octaves re f_{probe} (Fig. 8A, B). This agrees with the characteristics of two-tone suppression observed in auditory nerve fibers (Sachs and Kiang 1968), basilar membrane (Cooper 1996; Rhode 2007), and hair cells (Sellick and Russell 1979), indicating that the main site of two-tone suppression is located basal to the probe frequency's characteristic place. Increasing the probe level and decreasing the criterion resulted in shifting the SFOAE STC tip further away from the probe frequency toward higher frequencies, again reflecting the frequency and level dependence of SFOAE suppression functions (Brass and Kemp 1993; Keefe et al. 2008). In contrast, the frequency at the tip of PTC almost always coincided

with the probe frequency after taking into consideration the effects of masker sweep direction (Sęk et al. 2005; Sęk et al. 2007; Malicka et al. 2009). The discrepancy between f_{tip}s of PTCs and SFOAE STCs may reflect Delgutte's (1990b) observations that both suppression and spread of excitation play a role in simultaneous masking. Alternatively, the shift of f_{tip} of an SFOAE STC may not result purely from two-tone suppression characteristics, but may indicate that SFOAEs are generated in a region extending basally from the characteristic place of the probe frequency (Guinan 1990; Siegel et al. 2005; Choi et al. 2008).

Tuning Curve Parameters—Tip-to-Tail Ratio

OAE STCs have been used previously to estimate cochlear gain by calculating the tip-to-tail ratio (e.g., Mills 1998; Pienkowski and Kunov 2001; Gorga et al. 2003; Gorga et al. 2008; Gorga et al. 2011). In this study, tip-to-tail ratio was calculated from suppression thresholds near the f_{probe} and 0.6 octaves below f_{probe}. This likely underestimated the cochlear gain as tip-to-tail ratios reported here are 10–15 dB smaller than those observed for DPOAE STCs or SFOAE STCs calculated using thresholds ~1 octave below the probe frequency (Pienkowski and Kunov 2001; Gorga et al. 2008; Keefe et al. 2008; Gorga et al. 2011). Despite this difference we observed some expected patterns, i.e., a decrease in tip-to-tail ratio with increasing criterion, increasing probe level (at least for the 4000 SFOAE STCs) and decreasing probe frequency (Gorga et al. 2002; Gorga et al. 2003; Johnson et al. 2004; Gorga et al. 2008; Keefe et al. 2008; Gorga et al. 2011). The tip-to-tail ratios of PTCs were ~5–10 dB larger than those of SFOAE STCs, when compared at equivalent probe SL. This may indicate that PTCs are shaped in part by processes not reflected in OAEs, e.g., off-frequency listening (Johnson-Davies and Patterson 1979; Moore et al. 1984). As much as off-frequency listening could have contributed to the differences in tip-to-tail ratios between PTCs and STCs, it seems that it had only a minor influence on the shapes of PTCs around their tips as indicated by the good agreement between Q_{10}s obtained with the fast-PTC paradigm and a notched-noise paradigm in Fig. 13 (red and blue dashed lines).

The Shape of SFOAE STCs and Phase Effects—Implications for SFOAE Generation

Average SFOAE STCs transitioned from "V"-shaped curves to double-tipped curves with shallow high frequency slopes when decreasing the residual criterion and increasing the probe level for the 1,000-Hz probe but not for the 4,000-Hz probe (Fig. 2). Even more complex shapes were observed in individual data (Fig. 3). SFOAE STCs with shallow high frequency

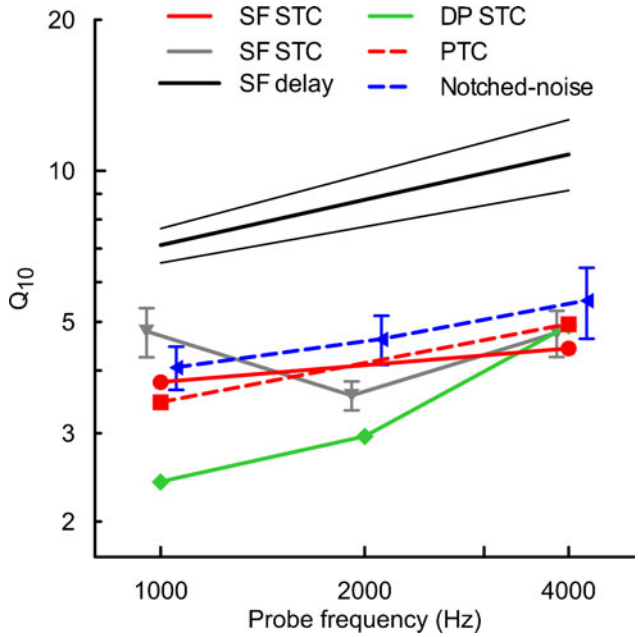

FIG. 13. Estimates of the sharpness of tuning in humans derived from different measurement methods, with the *solid lines* representing objective methods and *dashed lines* representing the behavioral methods. *Symbols* represent mean Q_{10} values (f_{tip}/BW10), and *error bars* denote ±1SE (if available). The *red lines* correspond to data from this report (Q_{10} for mean SFOAE STCs for the 10 dB SL/−6 dB SPL condition and mean PTCs are shown). *Black thick line* with 95 % CI (*thin lines*)—sharpness of tuning derived from SFOAE delays measured for a 40 dB SPL probe level (Shera et al. 2002); note: similar results were obtained by Bentsen et al. (2011); *gray line with inverted triangles*—SFOAE STCs recorded for a 40-dB SPL probe (Keefe et al. 2008); *green line with diamonds*—DPOAE STCs obtained at 10 dB SL as a function of the f_2 frequency (Gorga et al. 2011); *blue line with triangles*—simultaneous-masked notched-noise data obtained at 10 dB SL (Oxenham and Shera 2003). The Q_{ERB} reported in the above reports were converted to Q_{10} (where Q_{10}= $0.56Q_{ERB}$). Data are plotted offset along the *x* axis for clarity.

side slopes showing multiple inflections may be the result of contributions from generators located basal to the place of the probe frequency (Kemp and Chum 1980; Guinan 1990; Brass and Kemp 1993; Siegel et al. 2005; Choi et al. 2008) or contributions from a nonlinear distortion mechanism acting near the place of the suppressor frequency (Talmadge et al. 2000). The multiple inflections in STCs could also be related to subject-specific SFOAE generation characteristics contributing to SFOAE fine structure such as changes in cochlear reflectance along the basilar membrane (Zweig and Shera 1995).

Keefe et al. (2008) reported a similar phenomenon for SFOAE suppression sensitivity curves where a secondary peak of sensitivity emerged for higher probe levels, which they interpreted as indicating a qualitative change in cochlear nonlinearity rather than increased contribution from spatially distributed SFOAE sources or nonlinear distortion sources. Keefe et al. (2008) also observed relatively flat residual phase

curves, which supported the view that SFOAE are generated near the characteristic place of the probe. We also found that, on average, the residual phase did not vary substantially with suppressor frequency (Fig. 4). However, the individual phase curves demonstrated robust and repeatable phase shifts (Fig. 5 and 6) that changed consistently with measurement conditions (Fig. 7). The discrepancy between our observations and those of Keefe et al. may be due to the fact that we constructed tuning curves using a criterion of a fixed SFOAE residual instead of a fixed decrement in SFOAE amplitude. Comparisons of compound neural tuning curves built for either a fixed decrement criterion or a fixed residual criterion indicate that the latter approach results in better spatial representation of cochlear activity resulting from the stimulation by the probe, so that small contributions from restricted regions of the cochlea can be detected (Salt and Garcia 1990; Al'tman and Nikitin 2000). Thus, the fixed residual STC approach may be more sensitive for detecting contributions from spatially-distributed SFOAE sources (i.e., extending basal to probe characteristic place on the basilar membrane) which may explain the large fluctuations in phase for low residual criteria observed in this study. Suppressing a local sub-population of OAE generators may reveal a residual that meets a low criterion (i.e., the criterion can be met at relatively low suppressor levels). However, to meet a high residual criterion it would be necessary to sufficiently suppress a larger population of OAE generators, which would require increasing the suppressor levels, particularly for suppressor frequencies above the probe frequency (if the relative contribution of OAE generators decrease progressively from the probe characteristic place toward more basal locations). Thus, to satisfy the high criterion suppressors of different frequencies must suppress a similar population of OAE generators and the SFOAE residual phase curve should flatten. This view is also supported in our data by a significant increase in high-frequency slopes of STCs with increasing residual criterion. Large individual variability would be expected if the SFOAE results from interference between emission generators near the peak (where the phase of the probe excitation pattern varies steeply with distance) coupled with individual variation in the strength of the generators. However, our data do not allow us to distinguish whether the observed variations in SFOAE residual phase or STC shapes are due to the presence of spatially distributed generators or due to hypothesized distortion emissions evoked by the suppressor (Shera et al. 2004).

It is unlikely that the irregularity of SFOAE STC shapes was caused by random factors (i.e., noise, subject movements, SFOAE fluctuations) because we report good test-retest repeatability for both SFOAE STCs and PTCs. Thus, the irregularities in SFOAE STCs most likely reflect individual differences in SFOAE generation patterns, e.g., distribution of SFOAE sources along basilar membrane. In some cases, inflections may result from interactions with SOAEs (Fig. 3, see the triangles indicating the SOAE frequency aligning with a small inflection in STCs; also see Martin et al. 1988; Kummer et al. 1995). Although we tried to minimize the influence of such interactions by excluding subjects who had detectable SOAEs within ±350 Hz of f_{probe}, it is still possible that some SOAEs were present below our system noise floor or that SOAEs emerged due to acoustic stimulation (Burns et al. 1984).

Relating SFOAE STCs to Other Measures of Frequency Selectivity

SFOAE STCs demonstrate many characteristics typical of physiological tuning curves obtained in animals (e.g., Liberman and Kiang 1978; Sellick and Russell 1979; Robles and Ruggero 2001) as well as behavioral measures of frequency selectivity acquired in humans (e.g., Zwicker 1974). Narrow tuning, asymmetric shape, and increasing high frequency slopes with increasing frequency are all observed.

The average SFOAE STCs generally resembled the average PTCs, particularly for the lower probe levels and smaller residual criteria (Fig. 12, Table 3). This finding is consistent with other evidence that suppression plays an important role in simultaneous masking (Pickles 1984; Delgutte 1990b; Gifford and Bacon 2000; Rodriguez et al. 2010). Good agreement was found between PTCs (10 dB SL) and SFOAE STCs recorded at 20 dB SL for both probe frequencies, but at 30 dB SL there was a tendency for slightly larger error values (Table 3). Whether we would obtain better agreement between 20/30 dB SL SFOAE STCs and PTCs obtained at equivalent probe levels is hard to predict due to inconsistencies in the literature regarding the effects of probe level on sharpness of tuning of simultaneous-masking PTCs. For instance, Florentine et al. (1980) showed no consistent change in the sharpness of the PTC across a wide range of probe levels while Stelmachowicz and Jestead (1984) reported an increase in Q factor with increasing probe levels over a limited range of levels. Methodological differences between these studies (e.g., type of masker) might have caused the discrepancies. Nevertheless, 10 dB SL PTCs have been used consistently as a standard measure of behavioral tuning, justifying our methods.

The SFOAE STCs of Keefe et al. (2008) for 40 dB SPL probes (the lowest probe level for which data are available for both frequencies of interest) are in good

agreement with our STCs at 4,000 Hz; but at 1,000 Hz, their STCs appeared to be sharper (Fig. 13, compare red circles with gray inverted triangles). It is likely that discrepancies result from different approaches for building tuning curves, differences in probe levels, as well as individual differences in sharpness of tuning. The Qs derived from SFOAE iso-input curves (a fixed-level suppressor is swept in frequency around the probe) are smaller by roughly a factor of 0.6–0.7 as compared to data presented here (Bentsen et al. 2011) and this discrepancy is likely driven by differences in paradigms (Eustaquio-Martin and Lopez-Poveda 2011).

In humans, STCs have been measured much more commonly for DPOAEs (for review see Johnson et al. 2007). Although DPOAE STCs at 4,000 Hz reported previously (Gorga et al. 2011) appear to have tuning similar to the SFOAE STCs reported here, at 1,000 Hz the DPOAE STCs are almost twice as broad as the SFOAE curves we have measured (Fig. 13). This may be because DPOAEs are generated in multiple cochlear locations or in a broader generation region than SFOAEs (Shera and Guinan 1999; Knight and Kemp 2001; Martin et al. 2010). On the other hand, there appears to be agreement between the sharpness of tuning derived from SFOAE STCs and either SOAE STCs or TEOAEs in adults (Bargones and Burns 1988; Zizz and Glattke 1988; Zettner and Folsom 2003). This supports the view that SFOAEs are more closely related to either TEOAEs or SOAEs than to DPOAEs.

Another approach to derive cochlear tuning is based on SFOAE delays (Shera et al. 2002; Schairer et al. 2006; Lineton and Wildgoose 2009; Bentsen et al. 2011; Joris et al. 2011). Estimates of cochlear tuning by Shera et al. (2002) are much larger than our estimates derived from SFOAE STCs (Fig. 13), but Schairer et al. (2006) reported values that are closer to our estimates of tuning (at least at 4,000 Hz). The discrepancy between Qs derived from SFOAE latency by Shera et al. (2002) and Schairer et al. (2006) seems to originate in different approaches to data analysis (Bentsen et al. 2011; Shera and Bergevin 2012). Nevertheless, SFOAE STCs may indicate broader tuning than estimates derived from SFOAE delays due to the contribution of suppression to the STCs (Lineton and Wildgoose 2009; Bentsen et al. 2011).

Suppression tuning curves usually produce broader tuning than single-tone excitatory tuning curves for measurements of either basilar membrane, auditory nerve, or cochlear hair cells (Sachs and Kiang 1968; Sellick and Russell 1979; Rhode 2007); however, a contradictory result has been also reported (Cooper 1996). Thus, it is likely that SFOAE STCs underestimate human cochlear tuning. Similar issues with estimating frequency selectivity are applicable to behavioral measures of tuning, where the forward-masking paradigm is favored by some investigators over the simultaneous-masking paradigm (e.g., Oxenham and Shera 2003). Forward-masking experiments have been used to investigate cochlear function in humans (e.g., Rutten and Kuper 1982; Mason and Narula 1990; Oxenham and Plack 1997), even though its mechanisms are still not fully understood (e.g., Duifhuis 1973; Oxenham 2001) and it has been suggested that forward-masking occurs central to the cochlea (Relkin and Turner 1988; Nelson et al. 2009). Thus, both methods—simultaneous and non-simultaneous masking—have limitations in their applicability for investigating cochlear frequency selectivity. The fact that we found a close relationship between mean PTCs and mean SFOAE STCs suggest that the former are to a large extent shaped by cochlear mechanics (e.g., Pickles 1979; Evans 2001). This view is also supported by a good agreement between our estimates of sharpness of tuning and those obtained with evoked potential tuning curves (Eggermont 1977; Harrison et al. 1981; Harrison 1984; Markessis et al. 2009).

Limitations

The large variability in individual SFOAE STCs constitutes a major limitation for clinical application of this method to characterize an individual's frequency selectivity. It is also not clear how well SFOAE STCs would reflect changes in frequency selectivity due to hearing loss. Effects of cochlear insults on OAE suppression have been studied using DPOAEs and SOAEs but results have been inconclusive (Ruggero et al. 1983; Clark et al. 1984; Ruggero et al. 1984; Powers et al. 1995; Martin et al. 1998; Sun et al. 2000; Howard et al. 2002; Abdala and Fitzgerald 2003; Gorga et al. 2003; Howard et al. 2003; Gruhlke et al. 2012). Although SFOAE can be measured in hearing-impaired subjects (Ellison and Keefe 2005), it is not clear whether SFOAE STCs may provide a better measure of frequency selectivity in cases of cochlear insults.

The results from this study cannot be generalized to all normal hearing individuals because we included only participants who had recordable SFOAE responses to low level probe tones at both probe frequencies, and did not show SOAEs in the vicinity of either probe frequency. Indeed, our mean "total" SFOAE levels (Table 2) seemed to be slightly higher than previously reported median SFOAE levels obtained in normally hearing young adults at similar probe levels (Schairer et al. 2003; Schairer and Keefe 2005). The rationale behind such strict inclusion criteria was to (a) minimize possible interactions with SOAEs, (b) simplify statistical analyses, and (c) assess the effects of the probe level, specifically whether increasing the probe level, as would be necessary to record robust SFOAEs in both some normal- as well as

in hearing-impaired subjects, would compromise the estimation of frequency selectivity.

CONCLUSIONS

We conclude that SFOAE STCs are useful for estimating behavioral tuning noninvasively at the group level (e.g., Fig. 12), but not at the level of individual ears (e.g., Fig. 11). Gorga et al. (2011) reached a similar conclusion for estimating tuning with DPOAE STCs. The variability in SFOAE STCs recorded in our preselected subjects suggests that this procedure may not be useful in estimating frequency selectivity in a clinical setting.

ACKNOWLEDGMENTS

This work was supported by NIDCD grant DC006014 (P. Souza) Northwestern University and AAA Student Investigator Research Grant 2011 (K. Charaziak). We thank Sumitrajit Dhar for fruitful discussions and Kathleen Dunckley and James Dewey for comments on the manuscript.

REFERENCES

ABDALA C, FITZGERALD TS (2003) Ipsilateral distortion product otoacoustic emission (2f1-f2) suppression in children with sensorineural hearing loss. J Acoust Soc Am 114:919–931

AL'TMAN YA, NIKITIN NI (2000) Properties of derived cochlear action potentials in forward tonal masking in guinea pigs. Neurosci Behav Physiol 30:587–598

BARGONES JY, BURNS EM (1988) Suppression tuning curves for spontaneous otoacoustic emissions in infants and adults. J Acoust Soc Am 83:1809–1816

BENTSEN T, HARTE JM, DAU T (2011) Human cochlear tuning estimates from stimulus-frequency otoacoustic emissions. J Acoust Soc Am 129:3797–3807

BRASS D, KEMP DT (1993) Suppression of stimulus frequency otoacoustic emissions. J Acoust Soc Am 93:920–939

BURNS EM, STRICKLAND EA, TUBIS A, JONES K (1984) Interactions among spontaneous otoacoustic emissions. I. Distortion products and linked emissions. Hear Res 16:271–278

CHARAZIAK KK, SOUZA P, SIEGEL JH (2012) Time-efficient measures of auditory frequency selectivity. Int J Audiol 51:317–325

CHEATHAM MA, KATZ ED, CHARAZIAK KK, DALLOS P, SIEGEL JH (2011) Using stimulus frequency emissions to characterize cochlear function in mice. AIP Conf Proc 1403:383–388

CHOI YS, LEE SY, PARHAM K, NEELY ST, KIM DO (2008) Stimulus-frequency otoacoustic emission: measurements in humans and simulations with an active cochlear model. J Acoust Soc Am 123:2651–2669

CLARK WW, KIM DO, ZUREK PM, BOHNE BA (1984) Spontaneous otoacoustic emissions in chinchilla ear canals: correlation with histopathology and suppression by external tones. Hear Res 16:299–314

CLEVELAND WS (1979) Robust locally weighted regression and smoothing scatterplots. J Am Stat Assoc 74:829–836

CLEVELAND WS (1994) The elements of graphing data, Revth edn. AT&T Bell Laboratories, Murray Hill, N.J.

COOPER NP (1996) Two-tone suppression in cochlear mechanics. J Acoust Soc Am 99:3087–3098

DELGUTTE B (1990A) Two-tone rate suppression in auditory-nerve fibers: dependence on suppressor frequency and level. Hear Res 49:225–246

DELGUTTE B (1990B) Physiological mechanisms of psychophysical masking: observations from auditory-nerve fibers. J Acoust Soc Am 87:791–809

DREISBACH LE, SIEGEL JH, CHEN W (1998) Vector decomposition of distortion product otoacoustic emission sources in humans. Assoc Res Otolaryngol Abstr 21:347

DUIFHUIS H (1973) Consequences of peripheral frequency selectivity for nonsimultaneous masking. J Acoust Soc Am 54:1471–1488

EGGERMONT JJ (1977) Compound action potential tuning curves in normal and pathological human ears. J Acoust Soc Am 62:1247–1251

ELLIOT E (1958) A ripple effect in the audiogram. Nat Geosci 181:1076

ELLISON JC, KEEFE DH (2005) Audiometric predictions using stimulus-frequency otoacoustic emissions and middle ear measurements. Ear Hear 26:487–503

EUSTAQUIO-MARTIN A, LOPEZ-POVEDA EA (2011) Isoresponse versus isoinput estimates of cochlear filter tuning. J Assoc Res Otolaryngol 12:281–299

EVANS EF (2001) Latest comparisons between physiological and behavioural frequency selectivity. In: Breebaart J, Houtsma AJM, Kohlrausch A, Prijs VF, Schoonhoven R (eds) Physiological and Psychophysical Bases of Auditory Function. Maastricht, Shaker, pp 382–387

FLETCHER H (1940) Auditory patterns. Rev Mod Phys 12:47–65

FLORENTINE M, BUUS S, SCHARF B, ZWICKER E (1980) Frequency selectivity in normally-hearing and hearing-impaired observers. J Speech Hear Res 23:646–669

GIFFORD RH, BACON SP (2000) Contributions of suppression and excitation to simultaneous masking: effects of signal frequency and masker-signal frequency relation. J Acoust Soc Am 107:2188–2200

GORGA MP, NEELY ST, DORN PA, KONRAD-MARTIN D (2002) The use of distortion product otoacoustic emission suppression as an estimate of response growth. J Acoust Soc Am 111:271–284

GORGA MP, NEELY ST, KOPUN J, TAN H (2011) Distortion-product otoacoustic emission suppression tuning curves in humans. J Acoust Soc Am 129:817–827

GORGA MP, NEELY ST, DIERKING DM, DORN PA, HOOVER BM, FITZPATRICK DF (2003) Distortion product otoacoustic emission suppression tuning curves in normal-hearing and hearing-impaired human ears. J Acoust Soc Am 114:263–278

GORGA MP, NEELY ST, DIERKING DM, KOPUN J, JOLKOWSKI K, GROENENBOOM K, TAN H, STIEGEMANN B (2008) Low-frequency and high-frequency distortion product otoacoustic emission suppression in humans. J Acoust Soc Am 123:2172–2190

GRUHLKE A, BIRKHOLZ C, NEELY ST, KOPUN J, TAN H, JESTEADT W, SCHMID K, GORGA MP (2012) Distortion-product otoacoustic emission suppression tuning curves in hearing-impaired humans. J Acoust Soc Am 132:3292–3304

GUINAN JJ (1990) Changes in stimulus frequency otoacoustic emissions produced by two-tone suppression and efferent stimulation in cats. In: Dallos P, Geisler CD, Matthews JW, Ruggero MA, Steele CR (eds) The Mechanics and Biophysics of Hearing. Springer-Verlag, Madison, pp 170–177

HARRIS FP, PROBST R, XU L (1992) Suppression of the 2f1-f2 otoacoustic emission in humans. Hear Res 64:133–141

HARRISON RV (1984) Objective measures of cochlear frequency selectivity in animals and in man. A review. Acta Neurol Belg 84:213–232

HARRISON RV, ARAN JM, ERRE JP (1981) AP tuning curves from normal and pathological human and guinea pig cochleas. J Acoust Soc Am 69:1374–1385

Houtgast T (1972) Psychophysical evidence for lateral inhibition in hearing. J Acoust Soc Am 51:1885–1894

Howard MA, Stagner BB, Lonsbury-Martin BL, Martin GK (2002) Effects of reversible noise exposure on the suppression tuning of rabbit distortion-product otoacoustic emissions. J Acoust Soc Am 111:285–296

Howard MA, Stagner BB, Foster PK, Lonsbury-Martin BL, Martin GK (2003) Suppression tuning in noise-exposed rabbits. J Acoust Soc Am 114:279–293

Johnson-Davies D, Patterson RD (1979) Psychophysical tuning curves—restricting the listening band to the signal region. J Acoust Soc Am 65:765–770

Johnson TA (2010) Cochlear sources and otoacoustic emissions. J Am Acad Audiol 21:176–186

Johnson TA, Neely ST, Dierking DM, Hoover BM, Gorga MP (2004) An alternate approach to constructing distortion product otoacoustic emission (DPOAE) suppression tuning curves. J Acoust Soc Am 116:3263–3266

Johnson TA, Gorga MP, Neely ST, Oxenham AJ, Shera CA (2007) Relationships between otoacoustic and psychophysical measures of cochlear function. In: Manley GA, Fay RR, Popper AN (eds) Active processes and otoacoustic emissions in hearing. Springer, New York, pp 395–420

Joris PX, Bergevin C, Kalluri R, Mc Laughlin M, Michelet P, van der Heijden M, Shera CA (2011) Frequency selectivity in Old-World monkeys corroborates sharp cochlear tuning in humans. Proc Natl Acad Sci USA 108:17516–17520

Keefe DH, Ellison JC, Fitzpatrick DF, Gorga MP (2008) Two-tone suppression of stimulus frequency otoacoustic emissions. J Acoust Soc Am 123:1479–1494

Kemp DT, Chum RA (1980) Observations on the generator mechanism of stimulus frequency acoustic emissions–two tone suppression. In: deBoer E, Viergever MA (eds) Psychophysical, physiological and behavioral studies in hearing. Delft University Press, Delft, pp 34–41

Kemp DT, Brass D, Souter M (1990) Observations on simultaneous SFOAE and DPOAE generation and suppression. In: Dallos P, Geisler CD, Matthews JW, Ruggero MA, Steele CR (eds) The mechanics and biophysics of hearing. Springer, New York, pp 202–209

Kluk K, Moore BCJ (2004) Factors affecting psychophysical tuning curves for normally hearing subjects. Hear Res 194:118–134

Kluk K, Moore BCJ (2006) Detecting dead regions using psychophysical tuning curves: a comparison of simultaneous and forward masking. Int J Audiol 45:463–476

Knight RD, Kemp DT (2001) Wave and place fixed DPOAE maps of the human ear. J Acoust Soc Am 109:1513–1525

Koppl C, Manley GA (1993) Distortion-product otoacoustic emissions in the bobtail lizard. II: Suppression tuning characteristics. J Acoust Soc Am 93:2834–2844

Koppl C, Manley GA (1994) Spontaneous otoacoustic emissions in the bobtail lizard. II: Interactions with external tones. Hear Res 72:159–170

Kummer P, Janssen T, Arnold W (1995) Suppression tuning characteristics of the 2 f1-f2 distortion-product otoacoustic emission in humans. J Acoust Soc Am 98:197–210

Lee J, Dhar S, Abel R, Banakis R, Grolley E, Zecker S, Siegel J (2012) Behavioral hearing thresholds between 0.125 and 20 kHz using depth-compensated ear simulator calibration. Ear Hear 33:315–329

Liberman MC, Kiang NY (1978) Acoustic trauma in cats. Cochlear pathology and auditory-nerve activity. Acta Otolaryngol Suppl 358:1–63

Lineton B, Wildgoose CM (2009) Comparing two proposed measures of cochlear mechanical filter bandwidth based on stimulus frequency otoacoustic emissions. J Acoust Soc Am 125:1558–1566

Liu YW, Neely ST (2013) Suppression tuning of distortion-product otoacoustic emissions: results from cochlear mechanics simulation. J Acoust Soc Am 133:951–961

Long G (1998) Perceptual consequences of the interactions between spontaneous otoacoustic emissions and external tones. I. Monaural diplacusis and aftertones. Hear Res 119:49–60

Long GR (1984) The microstructure of quiet and masked thresholds. Hear Res 15:73–87

Long GR, Tubis A, Jones KL (1991) Modeling synchronization and suppression of spontaneous otoacoustic emissions using Van der Pol oscillators—effects of aspirin administration. J Acoust Soc Am 89:1201–1212

Malicka AN, Munro KJ, Baker RJ (2009) Fast method for psychophysical tuning curve measurement in school-age children. Int J Audiol 48:546–553

Margolis RH, Heller JW (1987) Screening tympanometry: criteria for medical referral. Audiology 26:197–208

Markessis E, Poncelet L, Colin C, Coppens A, Hoonhorst I, Kadhim H, Deltenre P (2009) Frequency tuning curves derived from auditory steady state evoked potentials: a proof-of-concept study. Ear Hear 30:43–53

Martin GK, Stagner BB, Lonsbury-Martin BL (2010) Evidence for basal distortion-product otoacoustic emission components. J Acoust Soc Am 127:2955–2972

Martin GK, Lonsburymartin BL, Probst R, Coats AC (1988) Spontaneous otoacoustic emissions in a nonhuman primate. 1. Basic features and relations to other emissions. Hear Res 33:49–68

Martin GK, Jassir D, Stagner BB, Lonsbury-Martin BL (1998) Effects of loop diuretics on the suppression tuning of distortion-product otoacoustic emissions in rabbits. J Acoust Soc Am 104:972–983

Mason SM, Narula AA (1990) A non-invasive electrophysiological technique for the measurement of 'tuning'. Clin Otolaryngol Allied Sci 15:43–48

Mills DM (1998) Interpretation of distortion product otoacoustic emission measurements. II. Estimating tuning characteristics using three stimulus tones. J Acoust Soc Am 103:507–523

Moore BC (1978) Psychophysical tuning curves measured in simultaneous and forward masking. J Acoust Soc Am 63:524–532

Moore BC, Glasberg BR, Roberts B (1984) Refining the measurement of psychophysical tuning curves. J Acoust Soc Am 76:1057–1066

Moore BCJ (2004) Frequency selectivity, masking, and the critical band. In: Moore BCJ (ed) An introduction to the psychology of hearing, 5th Edition. NY: Academic Press, pp 65–126.

Moore BCJ (2007) Cochlear hearing loss: physiological, psychological and technical issues, 2nd edn. Wiley, Chichester, UK

Neely S, Stevenson R (2002) SysRes. In: Technical Memorandum. Omaha, NE: Boys Town National Research Hospital.

Neely S, Liu Z (2011) EMAV: Otoacoustic Emission Averager. In: Technical Memorandum. Omaha, NE: Boys Town National Research Hospital.

Nelson PC, Smith ZM, Young ED (2009) Wide-dynamic-range forward suppression in marmoset inferior colliculus neurons is generated centrally and accounts for perceptual masking. J Neurosci 29:2553–2562

Oxenham AJ (2001) Forward masking: adaptation or integration? J Acoust Soc Am 109:732–741

Oxenham AJ, Plack CJ (1997) A behavioral measure of basilar-membrane nonlinearity in listeners with normal and impaired hearing. J Acoust Soc Am 101:3666–3675

Oxenham AJ, Shera CA (2003) Estimates of human cochlear tuning at low levels using forward and simultaneous masking. J Assoc Res Otolaryngol 4:541–554

Patterson RD (1976) Auditory filter shapes derived with noise stimuli. J Acoust Soc Am 59:640–654

Pickles JO (1979) Psychophysical frequency resolution in the cat as determined by simultaneous masking and its relation to auditory-nerve resolution. J Acoust Soc Am 66:1725–1732

PICKLES JO (1984) Frequency threshold curves and simultaneous masking functions in single fibres of the guinea pig auditory nerve. Hear Res 14:245–256

PIENKOWSKI M, KUNOV H (2001) Suppression of distortion product otoacoustic emissions and hearing threshold. J Acoust Soc Am 109:1496–1502

POWERS NL, SALVI RJ, WANG J, SPONGR V, QIU CX (1995) Elevation of auditory thresholds by spontaneous cochlear oscillations. Nat Geosci 375:585–587

RABINOWITZ WM, WIDIN GP (1984) Interaction of spontaneous otoacoustic emissions and external sounds. J Acoust Soc Am 76:1713–1720

RELKIN EM, TURNER CW (1988) A reexamination of forward masking in the auditory nerve. J Acoust Soc Am 84:584–591

RHODE WS (1971) Observations of the vibration of the basilar membrane in squirrel monkeys using the Mossbauer technique. J Acoust Soc Am 49(Suppl 2):1218

RHODE WS (2007) Mutual suppression in the 6 kHz region of sensitive chinchilla cochleae. J Acoust Soc Am 121:2805–2818

ROBINETTE MS, GLATTKE TJ (2007) Otoacoustic emissions: clinical applications, 3rd edn. Thieme, New York

ROBLES L, RUGGERO MA (2001) Mechanics of the mammalian cochlea. Physiol Rev 81:1305–1352

RODRIGUEZ J, NEELY ST, PATRA H, KOPUN J, JESTEADT W, TAN H, GORGA MP (2010) The role of suppression in psychophysical tone-on-tone masking. J Acoust Soc Am 127:361–369

RUGGERO MA, RICH NC (1991) Furosemide alters organ of corti mechanics: evidence for feedback of outer hair cells upon the basilar membrane. J Neurosci 11:1057–1067

RUGGERO MA, TEMCHIN AN (2005) Unexceptional sharpness of frequency tuning in the human cochlea. Proc Natl Acad Sci USA 102:18614–18619

RUGGERO MA, RICH NC, FREYMAN R (1983) Spontaneous and impulsively evoked otoacoustic emissions: indicators of cochlear pathology? Hear Res 10:283–300

RUGGERO MA, KRAMEK B, RICH NC (1984) Spontaneous otoacoustic emissions in a dog. Hear Res 13:293–296

RUGGERO MA, ROBLES L, RICH NC (1992) Two-tone suppression in the basilar membrane of the cochlea: mechanical basis of auditory-nerve rate suppression. J Neurophysiol 68:1087–1099

RUTTEN WL, KUPER P (1982) AP unmasking and AP tuning in normal and pathological human ears. Hear Res 8:157–178

SACHS MB, KIANG NY (1968) Two-tone inhibition in auditory-nerve fibers. J Acoust Soc Am 43:1120–1128

SALT AN, GARCIA P (1990) Cochlear action potential tuning curves recorded with a derived response technique. J Acoust Soc Am 88:1392–1402

SCHAIRER KS, KEEFE DH (2005) Simultaneous recording of stimulus-frequency and distortion-product otoacoustic emission input–output functions in human ears. J Acoust Soc Am 117:818–832

SCHAIRER KS, FITZPATRICK D, KEEFE DH (2003) Input–output functions for stimulus-frequency otoacoustic emissions in normal-hearing adult ears. J Acoust Soc Am 114:944–966

SCHAIRER KS, ELLISON JC, FITZPATRICK D, KEEFE DH (2006) Use of stimulus-frequency otoacoustic emission latency and level to investigate cochlear mechanics in human ears. J Acoust Soc Am 120:901–914

SCHLOTH E, ZWICKER E (1983) Mechanical and acoustical influences on spontaneous otoacoustic emissions. Hear Res 11:285–293

SELLICK PM, RUSSELL IJ (1979) Two-tone suppression in cochlear hair cells. Hear Res 1:227–236

SĘK A, MOORE BCJ (2011) Implementation of a fast method for measuring psychophysical tuning curves. Int J Audiol 50:237–242

SĘK A, WICHER A, DRGAS S (2007) A fast method for the determination of psychophysical tuning curves: further refining. Arch Acoust 32:707–728

SĘK A, ALCANTARA J, MOORE BCJ, KLUK K, WICHER A (2005) Development of a fast method for determining psychophysical tuning curves. Int J Audiol 44:408–420

SHERA CA (2004) Mechanisms of mammalian otoacoustic emission and their implications for the clinical utility of otoacoustic emissions. Ear Hear 25:86–97

SHERA CA, GUINAN JJ JR (1999) Evoked otoacoustic emissions arise by two fundamentally different mechanisms: a taxonomy for mammalian OAEs. J Acoust Soc Am 105:782–798

SHERA CA, BERGEVIN C (2012) Obtaining reliable phase-gradient delays from otoacoustic emission data. J Acoust Soc Am 132: 927–943

SHERA CA, GUINAN JJ JR, OXENHAM AJ (2002) Revised estimates of human cochlear tuning from otoacoustic and behavioral measurements. Proc Natl Acad Sci USA 99:3318–3323

SHERA CA, TUBIS A, TALMADGE CL, GUINAN JJ JR (2004) The dual effect of "suppressor" tones on stimulus-frequency otoacoustic emissions. Assoc Res Otolaryngol Abstr 27:538

SIEGEL JH (2007) Calibration of otoacoustic emission probes. In: Robinette MS, Glattke TJ (eds) Otoacoustic emissions: clinical applications, 3rd edn. Thieme, New York

SIEGEL JH, CERKA AJ, RECIO-SPINOSO A, TEMCHIN AN, VAN DIJK P, RUGGERO MA (2005) Delays of stimulus-frequency otoacoustic emissions and cochlear vibrations contradict the theory of coherent reflection filtering. J Acoust Soc Am 118:2434–2443

STELMACHOWICZ PG, JESTEADT W (1984) Psychophysical tuning curves in normal-hearing listeners: test reliability and probe level effects. J Speech Hear Res 27:396–402

SUN W, DING D, REYES S, SALVI RJ (2000) Effects of AC and DC stimulation on chinchilla SOAE amplitude and frequency. Hear Res 150:137–148

TALMADGE CL, TUBIS A, LONG GR, TONG C (2000) Modeling the combined effects of basilar membrane nonlinearity and roughness on stimulus frequency otoacoustic emission fine structure. J Acoust Soc Am 108:2911–2932

TASCHENBERGER G, MANLEY GA (1997) Spontaneous otoacoustic emissions in the barn owl. Hear Res 110:61–76

TASCHENBERGER G, MANLEY GA (1998) General characteristics and suppression tuning properties of the distortion-product otoacoustic emission 2f1-f2 in the barn owl. Hear Res 123:183–200

VOGTEN LL (1974) Pure-tone masking: a new result from a new method. In: Zwicker E, Terhardt E (eds) Facts and models in hearing; proceedings. Springer, Berlin, pp 142–155

WILSON JP (1980) Evidence for a cochlear origin for acoustic re-emissions, threshold fine-structure and tonal tinnitus. Hear Res 2:233–252

ZETTNER EM, FOLSOM RC (2003) Transient emission suppression tuning curve attributes in relation to psychoacoustic threshold. J Acoust Soc Am 113:2031–2041

ZIZZ CA, GLATTKE TJ (1988) Reliability of spontaneous otoacoustic emission suppression tuning curve measures. J Speech Hear Res 31:616–619

ZUREK PM (1981) Spontaneous narrowband acoustic signals emitted by human ears. J Acoust Soc Am 69:514–523

ZWEIG G, SHERA CA (1995) The origin of periodicity in the spectrum of evoked otoacoustic emissions. J Acoust Soc Am 98:2018–2047

ZWICKER E (1974) On a psychoacoustical equivalent of tunning curves. In: Zwicker E, Terhardt E (eds) Facts and models in hearing. Springer, Berlin, pp 132–140

ZWICKER E, WESEL J (1990) The effect of addition in suppression of delayed evoked otoacoustic emissions and in masking. Acta Acustica 70:189–196